CANCER

Control of brain tumor growth by reactivating myeloid cells with niacin

Susobhan Sarkar[1], Runze Yang[2]*, Reza Mirzaei[1]*, Khalil Rawji[1], Candice Poon[1], Manoj K. Mishra[1], Franz J. Zemp[3], Pinaki Bose[3,4,5], John Kelly[1,3], Jeff F. Dunn[1,2], V. Wee Yong[1,3]†

Glioblastomas are generally incurable partly because monocytes, macrophages, and microglia in afflicted patients do not function in an antitumor capacity. Medications that reactivate these macrophages/microglia, as well as circulating monocytes that become macrophages, could thus be useful to treat glioblastoma. We have discovered that niacin (vitamin B3) is a potential stimulator of these inefficient myeloid cells. Niacin-exposed monocytes attenuated the growth of brain tumor–initiating cells (BTICs) derived from glioblastoma patients by producing anti-proliferative interferon-α14. Niacin treatment of mice bearing intracranial BTICs increased macrophage/microglia representation within the tumor, reduced tumor size, and prolonged survival. These therapeutic outcomes were negated in mice depleted of circulating monocytes or harboring interferon-α receptor–deleted BTICs. Combination treatment with temozolomide enhanced niacin-promoted survival. Monocytes from glioblastoma patients had increased interferon-α14 upon niacin exposure and were reactivated to reduce BTIC growth in culture. We highlight niacin, a common vitamin that can be quickly translated into clinical application, as an immune stimulator against glioblastomas.

INTRODUCTION

Glioblastomas (GBMs) are the most malignant and common form of primary tumors that arise in the adult central nervous system (CNS). They are deadly tumors with a median survival of 14.6 months despite aggressive surgery, chemotherapy with temozolomide, and radiation (*1*). The prognosis for GBMs remains dismal, in part, because their stem-like cells, brain tumor–initiating cells (BTICs), are relatively resistant to chemoradiotherapy (*2*–*4*), in contrast to their more differentiated progenies. Further, BTICs account for glioma recurrence during temozolomide treatment in mice (*2*). Thus, there is an unmet need to develop therapeutics targeting BTICs.

An additional feature that contributes to the deadly nature of GBM is the tumors' efficient exploitation of their microenvironment, including of immune cells that infiltrate the tumor (*3*–*12*). The inflammatory infiltrate is dominated by peripherally derived macrophages and CNS-intrinsic microglia. These cells are histologically indistinguishable from each other and are collectively termed macrophages/microglia. The macrophages/microglia and circulating monocytes that become macrophages in tissues (collectively referred to here as myeloid cells) may initially attempt to control tumor growth but are ultimately subverted by BTICs and their progenies to assume an immunosuppressive phenotype and to promote GBM growth (*8*, *12*, *13*). Hence, medications that disable the tumor-promoting macrophages/microglia or those that reactivate the tumor-fighting properties of compromised circulating monocytes, in addition to tumor-infiltrating macrophages/microglia, are highly desired for GBMs.

There is immense interest in improving the prognosis of GBM by targeting monocytes, macrophages, and microglia. Approaches include deleting these populations by targeting their survival factor, colony-stimulating factor-1 (*14*, *15*); reducing their chemotaxis into tumor (*16*–*18*); using them as vehicles for drug delivery (*19*); depleting the number of immunosuppressive cells (*16*, *20*) or increasing the amount of proinflammatory cells (*21*–*23*); blocking immunosuppression by these cells (*24*); reprogramming or converting the immunosuppressive cells into proinflammatory types (*25*–*28*); or using pharmacological activators to produce stimulated phenotypes that curb tumor growth (*21*, *22*, *24*).

We previously screened a drug library of 1040 compounds and reported on those that inhibit microglia activity (*29*). In that screen, we also found compounds that further increased microglial inflammatory activity elicited by lipopolysaccharide (LPS) stimulation, as measured by elevation of tumor necrosis factor–α (TNF-α). Of these, amphotericin B, an antifungal medication, had considerable antitumor activity (*22*), but this medication is poorly tolerated in humans. Another compound that increased TNF-α in LPS-activated microglia in our screen was niacin (vitamin B3 or nicotinic acid) (*29*). Because niacin has been safely used in humans at high doses to treat atherosclerotic coronary disease and dyslipidemias (*30*–*32*), we investigated the hypotheses that niacin-stimulated myeloid cells would inhibit the growth of BTICs in culture and prolong the survival of mice with intracranial BTICs. Here, we report our findings that niacin is a promising treatment for the currently incurable GBMs.

RESULTS

Niacin promotes the stimulation of monocytes, macrophages, and microglia in culture

We first used mouse bone marrow–derived macrophages (BMDMs) to evaluate the activity of niacin. These cells were enriched from bone marrow cells that were exposed to macrophage colony-stimulating factor (MCSF) as described previously (*33*). After 10 days in MCSF-containing medium, more than 85% of the cells were macrophages,

[1]Department of Clinical Neurosciences and the Hotchkiss Brain Institute, University of Calgary, Calgary, Alberta T2N 4N1, Canada. [2]Department of Radiology and the Hotchkiss Brain Institute, University of Calgary, Calgary, Alberta T2N 4N1, Canada. [3]Department of Oncology and the Arnie Charbonneau Cancer Institute, University of Calgary, Calgary, Alberta T2N 4N1, Canada. [4]Department of Biochemistry and Molecular Biology, University of Calgary, Calgary, Alberta T2N 4N1, Canada. [5]Department of Surgery, University of Calgary, Calgary, Alberta T2N 4N1, Canada.
*These authors contributed equally to this work.
†Corresponding author. Email: vyong@ucalgary.ca

as determined by F4/80$^+$, CD11b$^+$, and CD45$^+$ cells (fig. S1) and by Iba1 immunoreactivity (Fig. 1A). Less than 10% of the BMDM cultures were Ly6C$^+$ monocytes or Ly6G$^+$ neutrophils (fig. S1). Twenty percent to 30% of the macrophages expressed CD11c and MHCII (major histocompatibility complex II), 60 to 80% expressed the costimulatory markers CD80 and CD86, and 95% were CD206$^+$. We did not detect any F4/80^{Low}CD11b^{Low} dendritic cells in the BMDM cultures (fig. S1).

In our published drug screen, we found that niacin (10 μM, given 1 hour before LPS treatment) produced more TNF-α (146%) than LPS alone (100%) (*29*). Here, we first asked whether niacin alone could increase cytokines in naive BMDMs or whether it required a priming stimulus. BMDMs were incubated with 100 μM niacin because this concentration is readily achieved in humans taking 1 g of niacin for dyslipidemia (mean range in serum of 120 to 230 μM between 1 and 2 hours after intake) (*34*). Niacin by itself did not increase TNF-α and other cytokines in the cell-conditioned medium collected after 24 hours, but it further promoted TNF-α, interleukin-6 (IL-6), IL-12, and CXCL10 secretion elicited by LPS (Fig. 1B and fig. S2). In contrast, niacin reduced a major immunosuppressive molecule in GBMs, IL-10 (Fig. 1B) (*35*).

Previous studies referred to niacin as an anti-inflammatory factor that lowered the activity of stimulated macrophages (*36*, *37*). To resolve the discrepancy, we pretreated BMDMs with supraphamacologic concentrations of niacin (500 and 1000 μM) 24 hours before LPS stimulation as conducted in the contradictory reports and compared this to obtainable in vivo niacin concentrations and a 1-hour pretreatment. Notably, 10 and 100 μM niacin added 1 hour before LPS elicited an increase in TNF-α, whereas higher niacin concentrations decreased this cytokine; a 24-hour pretreatment with all niacin concentrations lowered the subsequent LPS effect (Fig. 1C). Thus, niacin stimulates, rather than inhibits, LPS-activated macrophages at pharmacologically relevant in vivo concentrations when given 1 hour before LPS. Recently, a study in Parkinson's disease patients found that niacin shifted macrophages from a proinflammatory to an anti-inflammatory phenotype (*38*); however, these authors used 100 to 250 mg of niacin, whereas gram quantities are used in dyslipidemia.

During the culture period for BMDMs, some cells remained floating as monocytes (*39*). These were collected and exposed to 100 μM niacin for 24 hours. We noted that the viability and differentiation of these monocytes were largely unaffected by niacin, with the exception of the increase in mean fluorescence intensity of CD80 (fig. S3).

We tested whether niacin stimulation occurred with different immune cell types from multiple species. Human blood-derived monocytes, human monocyte-matured macrophages, and brain-derived microglia, as well as mouse peritoneal macrophages and BMDMs, did not increase TNF-α in response to niacin alone, but all promoted the TNF-α secretion elicited by LPS (Fig. 1D). Moreover, using the less potent but endogenously produced activators interferon-γ (IFN-γ)

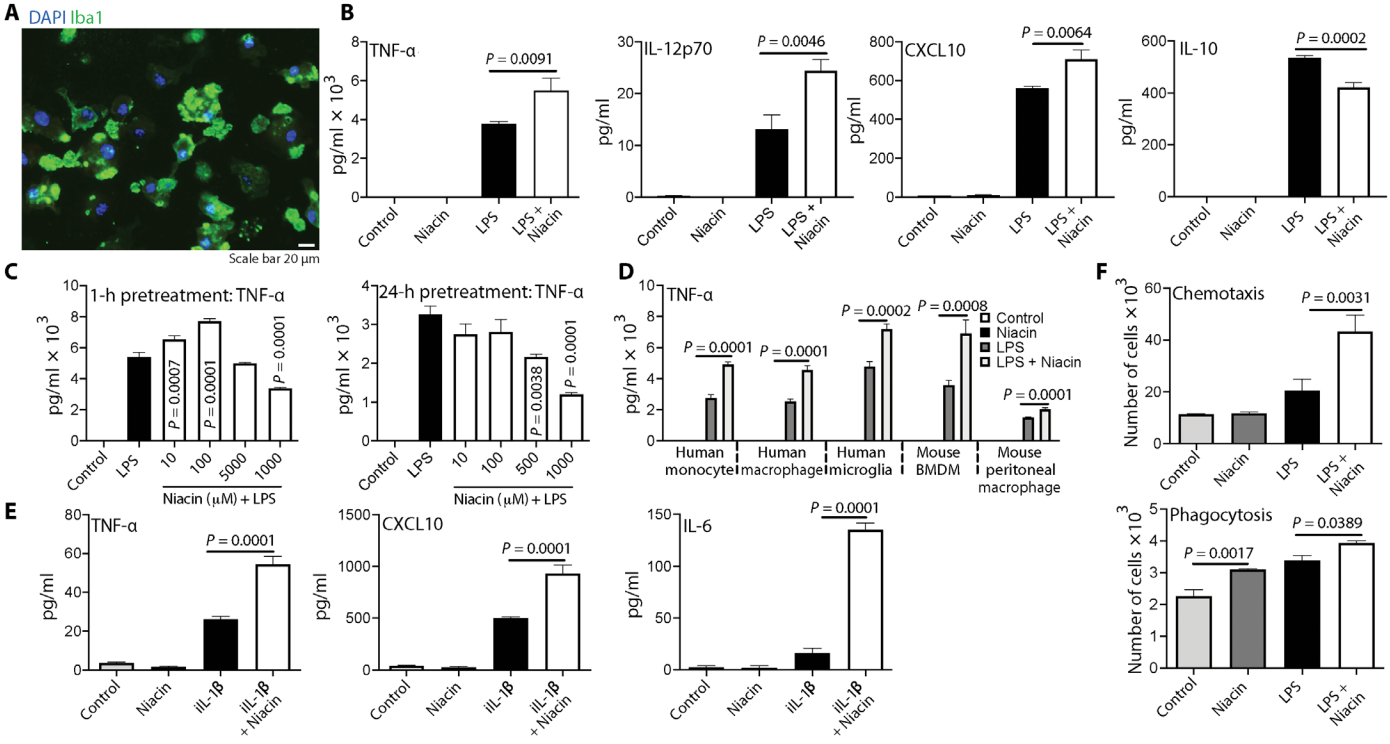

Fig. 1. Niacin stimulates monocytes, macrophages, and microglia. (**A**) Mouse bone marrow–derived macrophages (BMDMs) were cultured to over 85% purity as determined by Iba1 fluorescence. (**B**) Cytokine and chemokine expression by BMDMs treated with LPS (100 ng/ml) and/or niacin (100 μM). (**C**) TNF-α concentration with pharmacologic concentrations of niacin in mouse BMDMs when given 1 or 24 hours before LPS. (**D**) TNF-α concentration upon treatment of human monocytes, macrophages, and microglia and mouse BMDMs and peritoneal macrophages with niacin (100 μM) alone or niacin (100 μM) plus LPS (100 ng/ml). (**E**) TNF-α, CXCL10, and IL-6 concentrations upon treatment with interferon-γ (IFN-γ) and IL-1β (iIL-1β) in BMDMs in the presence or absence of niacin. (**F**) Effect of niacin on chemotaxis and phagocytosis in LPS-activated BMDMs or without LPS. All bars are means ± SEM of quadruplicate cultures, and data were analyzed by one-way ANOVA with Dunnett's post hoc test relative to the LPS group; only the *P* values for differences between LPS and LPS + niacin are displayed.

and IL-1β (collectively abbreviated as iIL-1β), the amounts of TNF-α, CXCL10, and IL-6 (Fig. 1E) raised in BMDMs by iIL-1β were further enhanced by 1-hour pretreatment with 100 μM niacin, as were the chemokines CCL2 and CCL5 (fig. S2); however, a noticeable increase in CCL3 and CCL4 was observed with niacin treatment without priming by iIL-1β (fig. S2).

We exposed BMDMs to IL-4, a common stimulus that increases "M2"-like characteristics, to determine whether niacin would affect macrophage polarization under this condition. Attempts to measure an immunosuppressive cytokine, transforming growth factor–β1 (TGF-β1), in the conditioned medium of cells were unsuccessful because its amounts were below detection. Arginase activity was measurable, and the arginase activity increased by IL-4 in BMDMs was not affected by niacin (fig. S2C).

We addressed whether niacin affected other aspects of LPS-stimulated macrophage activity and found that it promoted chemotaxis and phagocytosis of LPS-exposed cells (Fig. 1F). We noted that niacin alone promoted phagocytosis by naive BMDMs (Fig. 1F), thus indicating that some responses of myeloid cells can be independently triggered by niacin without LPS priming.

In summary, niacin increases the amounts of several cytokines and chemokines in monocytes, macrophages, and microglia primed by LPS or iIL-1β. For phagocytosis, niacin increased this activity without the necessity of LPS priming.

Niacin-treated monocytes reduce the growth of GBM patient–derived BTICs in vitro

We used nine human BTIC lines generated in-house from resected GBM specimens (*40*–*45*). Cells were plated at either 5000 or 10,000 per well in 96-well plates and exposed for 7 or 3 days, respectively, to conditioned medium collected from monocytes of healthy human volunteers. We focused on monocytes among myeloid cells because monocytes would be exposed to niacin while circulating in blood before their infiltration into tumors as macrophages; moreover, the capacity of niacin to cross the intact blood-brain barrier is not clear (*46*), although niacin is detected in the brain after intravenous administration (*47*) in humans and the blood-brain barrier may be disrupted in GBM patients (*48*).

Whereas BTICs in control conditions formed prominent spheres over a 3- or 7-day period, this was reduced by monocyte conditioned medium (MonoCM) from healthy adults; notably, the sphere growth was further attenuated by medium from niacin-treated monocytes (Niacin-MonoCM) (Fig. 2, A and B, and fig. S4A). Notably, BT048 and BT53M extensively used in most of the vitro and in vivo experiments were of divergent genetic backgrounds (fig. S4B). In addition, O6-methylguanine-DNA methyltransferase (MGMT)–methylated (thus temozolomide-sensitive) patient-derived BTIC lines (BT048, BT084, BT206, and BT53M) and MGMT-unmethylated (temozolomide-resistant) lines (BT012, BT030, BT073, and BT075) (*43*) were all sensitive to inhibition by Niacin-MonoCM (Fig. 2A and fig. S4A).

Extreme limiting dilution assay further confirmed the potent growth-reducing effects of Niacin-MonoCM on BTICs (fig. S5A). These results emphasize that niacin can alter monocytes directly to reduce BTIC growth; specifically, the Niacin-MonoCM reduced cell cycling and induced apoptosis of BTICs and caused BTICs to differentiate, as suggested by lowered expression of the stemness markers nestin, Sox2, and musashi-1 (Fig. 2C and fig. S5, B to D).

When large BTIC spheres formed over several days in culture, the application of Niacin-MonoCM promptly reduced the size of the spheres (fig. S6A). Because niacin by itself was not toxic and ineffective in containing BTIC growth (fig. S6, B and C), we conclude that its effects on BTICs require the monocyte intermediary.

Mechanisms by which niacin-treated monocytes reduce BTIC growth in culture

We performed microarray analyses [Gene Expression Omnibus (GEO) accession number GSE103381] for 39,000 genes on human monocytes isolated from three healthy volunteers. The volunteers' blood-derived monocytes were exposed to niacin (100 μM) ex vivo for 6 hours. Principal components analysis indicated that there was divergence in the basal (untreated) transcriptome of monocytes from all three participants, and niacin treatment resulted in changes unique to each individual (Fig. 2D); however, we also found 351 genes that were commonly altered after niacin treatment in all three participants with a cutoff of 1.2-fold (Fig. 2E); of these, 105 and 246 genes were up- and down-regulated, respectively, by niacin (data file S1). We note that the fold change of gene transcripts in response to niacin alone is modest, but this bodes well for its good tolerance in humans.

Because the conditioned medium from niacin-stimulated monocytes reduced BTIC growth, we next addressed which of the altered genes encoded soluble molecules, using cellular component ontology analysis in the PANTHER database, where genes are categorized based on their cellular localization (fig. S6D). Among the different categories, we selected the extracellular region, aligned with our interest in secreted proteins. We identified seven extracellular genes that were up-regulated by niacin across monocyte cultures (Fig. 2F), including IFN-α14, which was reported to decrease proliferation of transformed renal and lymphoid cells in culture in a single study (*49*). Other IFN-α were not altered in niacin-treated monocytes (data file S1). We confirmed the increase in IFN-α14 by niacin through real-time polymerase chain reaction (PCR) of two additional human monocyte cultures (Fig. 2G). Moreover, niacin (100 μM) treatment of monocytes from five healthy individuals increased their amount of IFN-α14 protein in cell-conditioned medium (Fig. 2H). We noted that LPS did not enhance the niacin-stimulated increase of IFN-α14 protein (fig. S6E).

The finding that niacin treatment of monocytes increased IFN-α14 led us to ask whether this type I IFN could inhibit BTIC growth. The addition of recombinant human IFN-α14 reduced BTIC sphere formation within a concentration range of 5 to 100 ng/ml but not at 1 ng/ml or below (Fig. 3A and fig. S6F). Moreover, recombinant human IFN-α14 reduced the S-phase of the cell cycle of BTICs (Fig. 3B). We detected the up-regulation of IFN-α–responsive genes, such as *IRF9*, *STAT1*, and *STAT2*, in three human BTIC lines with IFN-α14 treatment (Fig. 3, C and D, and data file S2). Last, we found that recombinant murine IFN-α14 (mIFN-α14) also reduced sphere formation by human BTICs (fig. S7); this cross-species capacity provides the rationale to treat mice harboring intracranial human BTICs with niacin, because mIFN-α14 produced by monocytes and macrophages in vivo may conceivably work on the human implants.

To link the niacin-induced IFN-α14 secretion by monocytes to suppression of BTIC growth, it would be desirable to prevent the production or release of IFN-α14 by monocytes. However, primary monocytes did not survive transient RNA interference (RNAi) approaches such as small interfering RNA (siRNA) or lentivirus. Moreover, two commercial antibodies blocking the function of IFN-α14 killed cells and thus could not be used. We therefore targeted BTICs to reduce their expression of the receptor for IFN-α14, the type 1

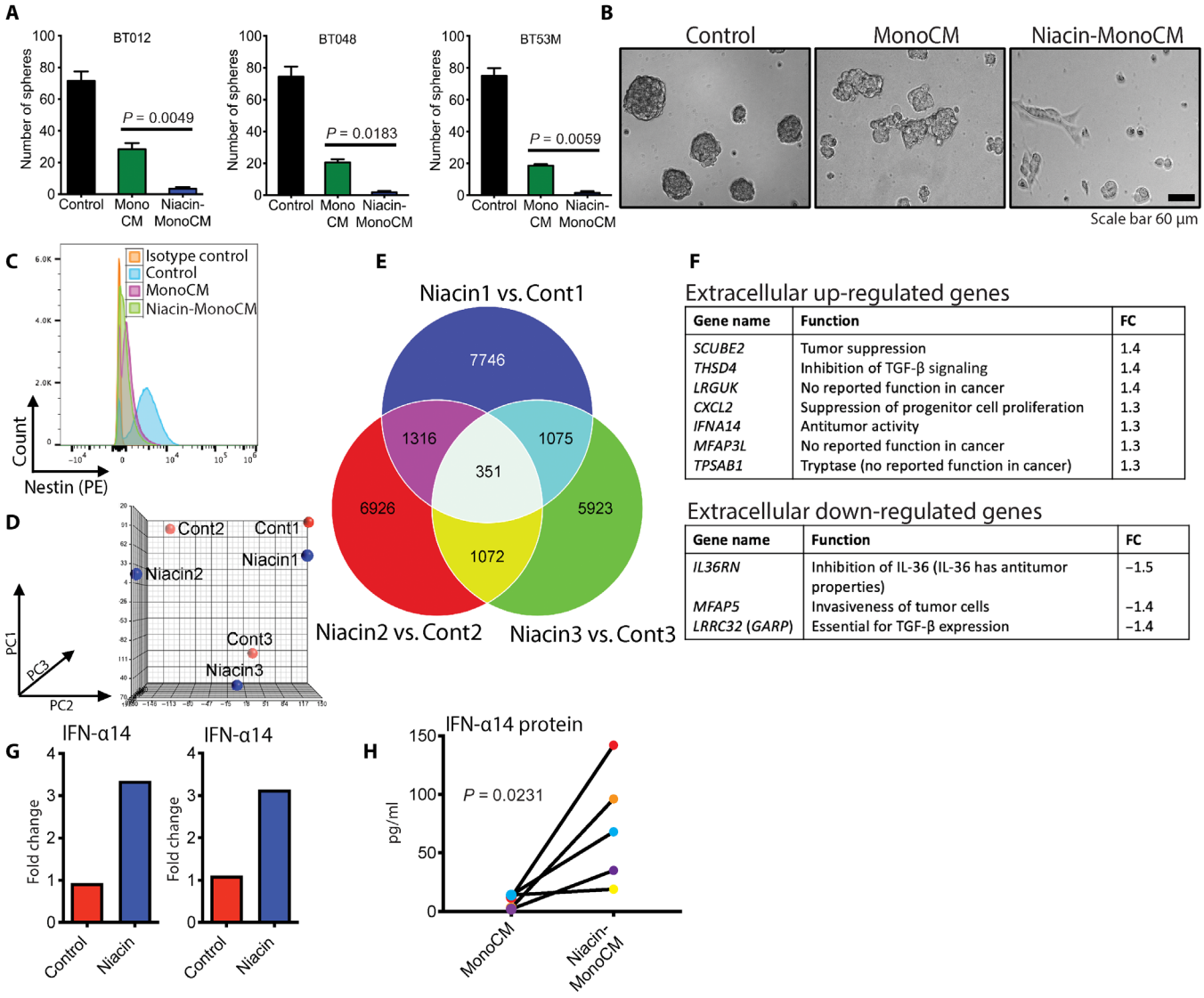

Extracellular up-regulated genes

Gene name	Function	FC
SCUBE2	Tumor suppression	1.4
THSD4	Inhibition of TGF-β signaling	1.4
LRGUK	No reported function in cancer	1.4
CXCL2	Suppression of progenitor cell proliferation	1.3
IFNA14	Antitumor activity	1.3
MFAP3L	No reported function in cancer	1.3
TPSAB1	Tryptase (no reported function in cancer)	1.3

Extracellular down-regulated genes

Gene name	Function	FC
IL36RN	Inhibition of IL-36 (IL-36 has antitumor properties)	−1.5
MFAP5	Invasiveness of tumor cells	−1.4
LRRC32 (*GARP*)	Essential for TGF-β expression	−1.4

Fig. 2. Niacin-treated monocytes reduce BTIC growth through soluble mediators including IFN-α14. (**A**) Numbers of spheres above 60 μm diameter in three GBM patient–derived BTIC lines exposed to MonoCM or Niacin-MonoCM from healthy volunteers (one-way ANOVA with Tukey's post hoc test). (**B**) Images of 72-hour outcomes of spheres from a BT048 experiment; scale bar, 60 μm. (**C**) Fluorescence-activated cell sorting (FACS) analysis of stemness marker, nestin, in BTICs treated with MonoCM or Niacin-MonoCM. (**D**) Principal components analysis of microarray data of monocytes from three individuals under control or 6-hour niacin-stimulated conditions. (**E**) Venn diagram displaying the number of transcripts differentially and commonly altered by niacin between the three individuals. (**F**) Genes encoding secreted factors that were up- or down-regulated by niacin across three monocyte preparations. FC, fold change. (**G**) PCR quantification of IFN-α14 after 3 hours of exposure to niacin in monocytes from two additional subjects. (**H**) IFN-α14 protein concentration in the conditioned medium (CM) of monocytes from five control subjects under basal conditions (MonoCM) or niacin stimulation (Niacin-MonoCM) (paired *t* test, each line represents a single subject).

IFN-α receptor (IFNAR1), using siRNAs (Fig. 3E). In human BTIC lines with siRNA knockdown of IFNAR1, IFN-α14 (Fig. 3F) or Niacin-MonoCM (Fig. 3G) was no longer effective in reducing growth. These results support the contention that IFN-α14 produced by monocytes helps account for the attenuation of BTIC growth by niacin-exposed monocytes.

We interrogated three separate GBM databases [GEO accession numbers GSE4536 and GSE7696, and The Cancer Genome Atlas (TCGA)] and found that *IFNA14* transcript was expressed at very low and comparable amounts in normal brain and GBM samples and that its amount did not influence longevity of patients (fig. S8). We also interrogated the TCGA database for other soluble factors (*SCUBE2*, *THSD4*, *LRGUK*, *CXCL2*, and *LRRC32*) altered upon niacin treatment and found that these did not associate with survival of patients either (fig. S9).

Niacin prolongs longevity of SCID mice with intracranial patient-derived BTICs

We implanted GBM patient–derived BT012 cells into the right striatum of severe combined immunodeficient (SCID) mice and initiated 7 days of systemic intraperitoneal treatment with niacin or vehicle. Niacin was used at 100 mg/kg because a previous study found that this dose produces 100 to 250 μM plasma concentration in mice between 1 and 9 hours (*50*). The therapeutic efficacy of niacin was first

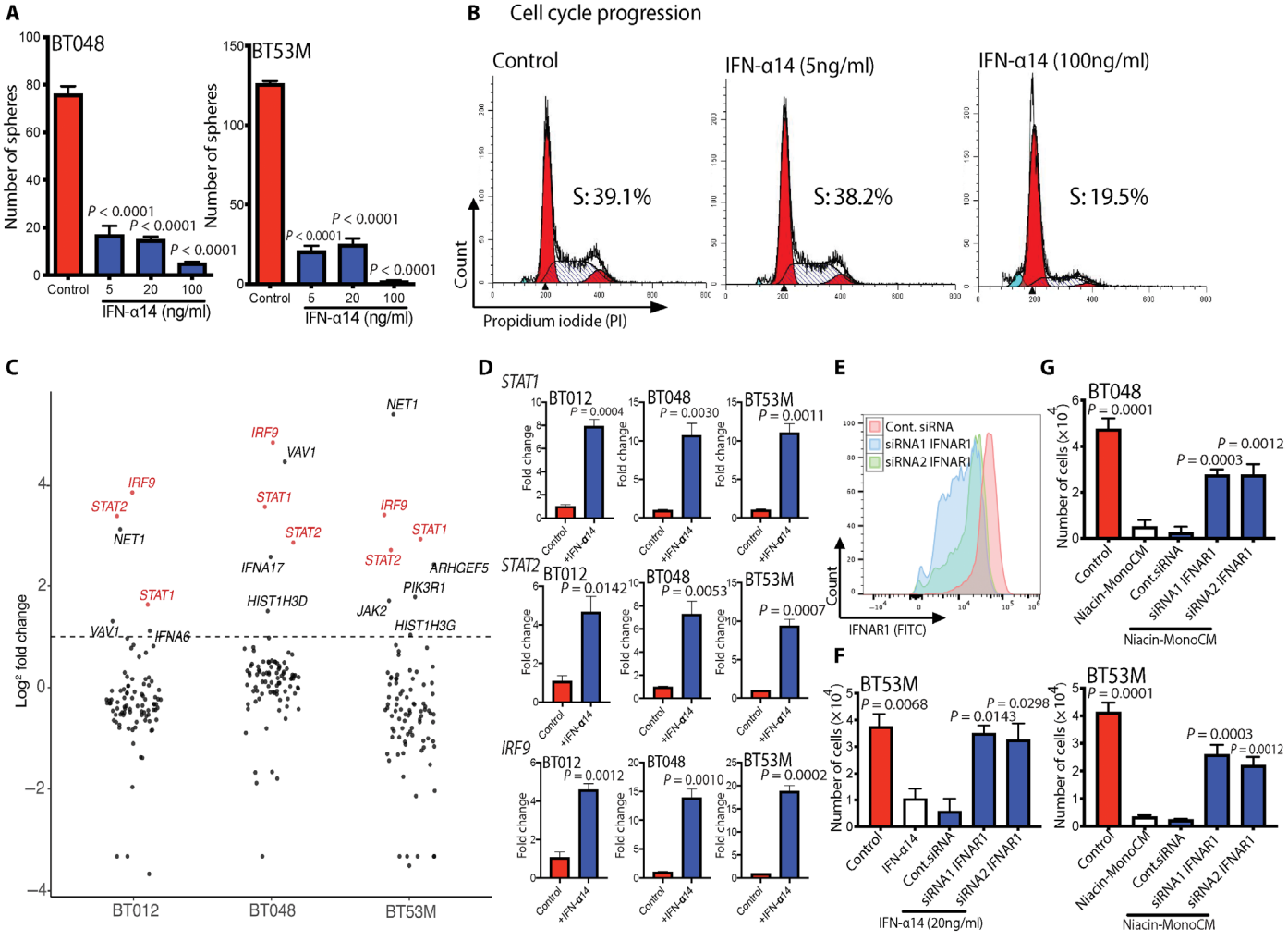

Fig. 3. IFN-α14 and induction of type I IFN-responsive genes in BTICs. (**A**) Effect of recombinant IFN-α14 on BT048 and BT53M growth at 72 hours; one-way ANOVA compared to control. (**B**) Cell cycle analysis by propidium iodide flow cytometry in human BT53M cells incubated with recombinant human IFN-α14; the numbers refer to the percentage of cells in the S phase of the cell cycle. (**C**) TaqMan Array Human Interferon Pathway analysis of IFN-responsive genes upon treatment with IFN-α14 in three human BTIC lines. (**D**) PCR validation of IFN-responsive genes *STAT1*, *STAT2*, and *IRF9* in three human BTIC lines upon IFN-α14 treatment; unpaired *t* test compared to control. (**E**) Validation of IFNAR1 protein expression in BT53M cells transfected with two siRNAs to IFNAR1, 48 hours after transfection. Effect of recombinant IFN-α14 (**F**) or Niacin-MonoCM (**G**) on sphere-forming capacity of IFNAR1 knockdown BTIC cells; one-way ANOVA with Tukey's post hoc comparisons. All bars are means ± SEM of quadruplicate cultures.

assessed 6 weeks after implantation in live asymptomatic animals using T2*-weighted magnetic resonance imaging (MRI). Images showed large tumors in vehicle-treated mice and a much reduced tumor volume with niacin (Fig. 4, A and B). Vehicle-treated mice became symptomatic (lethargic, fluffed fur) shortly thereafter, and Kaplan-Meier survival plots showed that niacin prolonged survival (Fig. 4C).

We also used MRI to determine the effect of niacin on monocyte/macrophage infiltration into implanted tumors. Here, the contrast agent USPIO (ultrasmall superparamagnetic iron oxide, ferumoxytol) was intravenously injected into mice, whereupon circulating phagocytes (largely monocytes) engulfed the iron particles; upon their migration into tumors, the iron signal could be tracked by MRI using changes in T_2* (*51*). In mice 46 days after implantation with BT048, we found no difference in tumor T_2* before and after ferumoxytol administration for vehicle-treated animals. However, there was a decrease in tumor T_2* indicative of ferumoxytol being trafficked into the tumor by monocytes after niacin treatment (Fig. 4, D and E). In corroboration, there was increased immunoreactivity for the macrophage/microglia marker Iba1 (Fig. 4F).

Next, we addressed the requirement for myeloid cells for reduction of tumor growth in niacin-treated mice. We implanted BT048 into the brains of SCID mice and reproduced the finding that daily niacin treatment prolonged the life span of mice (Fig. 4G). In parallel, other groups received weekly intravenous infusions of liposomes containing clodronate (dichloromethylene bisphosphonate) or phosphate-buffered saline (PBS) (control) starting at 7 days after implantation to deplete circulating monocytes and monocyte-derived macrophages (*52*); whether microglia were affected remained unclear. Effective depletion of monocytes/macrophages by clodronate liposomes in the livers of treated mice was observed by intravital microscopy (fig. S10). Niacin prolonged survival in mice treated

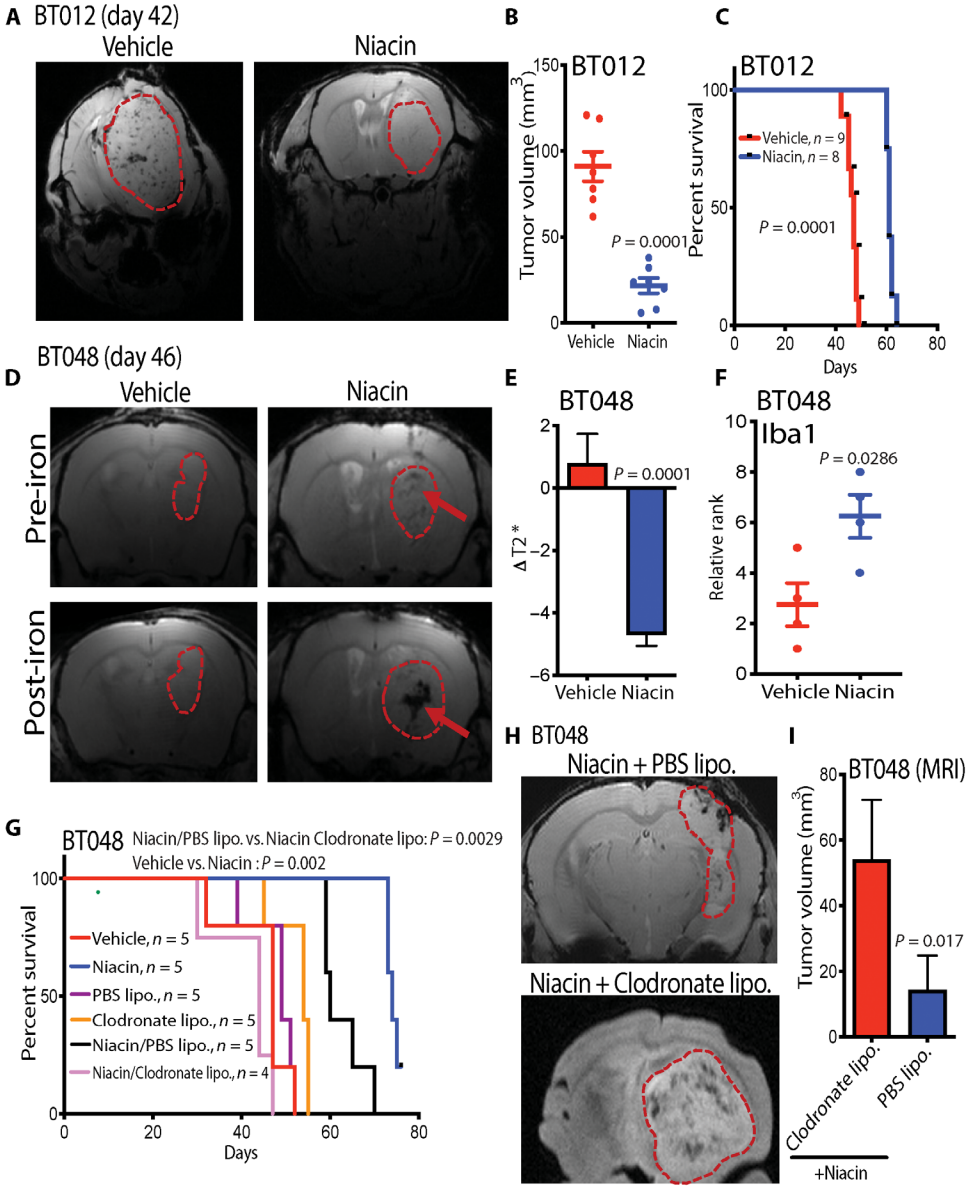

Fig. 4. Niacin reduces the intracranial growth of GBM patient–derived BTIC implants in immunodeficient mice and prolongs their life span. (**A** and **B**) Mice were implanted with 10,000 BT012 cells in the striatum. Niacin (100 mg/kg) or vehicle (saline) daily intraperitoneal treatment was initiated from day 7. Representative T2-weighted MRI images at day 42 (tumor demarcated with red outline) are shown in (A), with tumor volume across mice displayed in (B) (unpaired *t* test). (**C**) Kaplan-Meier analysis of survival of mice receiving vehicle or niacin therapy (log-rank test). (**D** and **E**) Mice implanted with BT048 cells were left undisturbed for 35 days, after which the animals were treated with either vehicle or niacin ($n = 4$ each) for 7 to 9 days. MRI was then conducted, and a baseline T_2* map ("pre-iron") was collected. Ferumoxytol was next given through the tail vein at a dose of 30 mg/kg as a 100-μl bolus, and another T_2* map ("post-iron") was collected 24 hours after. Representative MRI results (D) show darkening (arrow) after ferumoxytol injection only in the niacin-treated animals, indicating iron influx and thus monocyte infiltration (*51*) into the tumor (*t* test); the corresponding change in T2* is shown in (E). (**F**) After iron imaging [from (D)], mice were euthanized for immunohistochemistry to quantify Iba1-positive cells. (**G**) SCID mice were implanted with BT048 cells and initiated on daily niacin (100 mg/kg, intraperitoneally) or vehicle from day 7. Subsets of the niacin group were administered liposomes containing clodronate to deplete monocytes or liposomes containing PBS control. The Kaplan-Meier analysis ($n = 5$ per group) shows the therapeutic effect of niacin ($P = 0.002$ compared to vehicle, log-rank test) and the loss of niacin efficacy in clodronate liposome–treated mice compared to PBS liposome–treated animals. (**H** and **I**) Corresponding MRI images (H) and quantitation (I) (unpaired *t* test; $n = 4$ for clodronate liposome group and $n = 5$ for PBS liposome animals).

with niacin plus PBS-liposomes, but mice treated with clodronate liposomes no longer showed improved survival in the presence of niacin (Fig. 4G). MRI images showed large tumors in niacin + clodronate liposome–treated mice compared to those given niacin plus PBS-liposomes (Fig. 4, H and I). Thus, the efficacy of niacin required the presence of myeloid cells.

Niacin extends survival in immunocompetent mice with syngeneic BTICs

We extended our studies to syngeneic mice with normal immunity. We used the mBT0309 mouse BTIC line in the C57BL/6 background, previously generated and propagated as stem-like cells (*53*). In immunocompetent mice implanted with the mBT0309 line, niacin treatment extended survival, with this benefit lost in mice treated with clodronate but not PBS liposomes (Fig. 5, A to C). Thus, as with SCID mice implanted with patient-derived BTICs, the efficacy of niacin in immunocompetent mice with syngeneic brain grafts required myeloid cells. Immunohistochemistry of brain sections from niacin-treated immunocompetent mice showed reduced numbers of CD204/CD206 anti-inflammatory $Iba1^+$ macrophages/microglia (Fig. 5, D and E) compared to vehicle controls. Moreover, niacin-treated mice had detectable cleaved caspase 3 apoptotic cells in different areas of the tumor, whereas this was not readily apparent in vehicle-treated mouse brains (Fig. 5F).

Within the systemic circulation, determination of other immune cell types in niacin-treated mice showed that it did not affect $CD3^+$, $CD4^+$, $CD8^+$, or memory T cells; there was no substantial decrease in the number of regulatory T cells ($P = 0.058$) (fig. S11). Consistent with this, we did not find any difference in the $CD3^+$ cells in brain sections from niacin-treated mice compared to vehicle (fig. S11C).

We sought to determine whether the therapeutic efficacy of niacin in vivo involved signaling through the IFN-α14–IFNAR1 axis. We could not stably delete IFN-α14 from monocytes as noted earlier, so we generated IFNAR1 knockout (KO) mouse BTICs using the parental BT0309 line and the CRISPR gene editing system. DNA sequencing results show that the mouse *Ifnar1* gene was completely

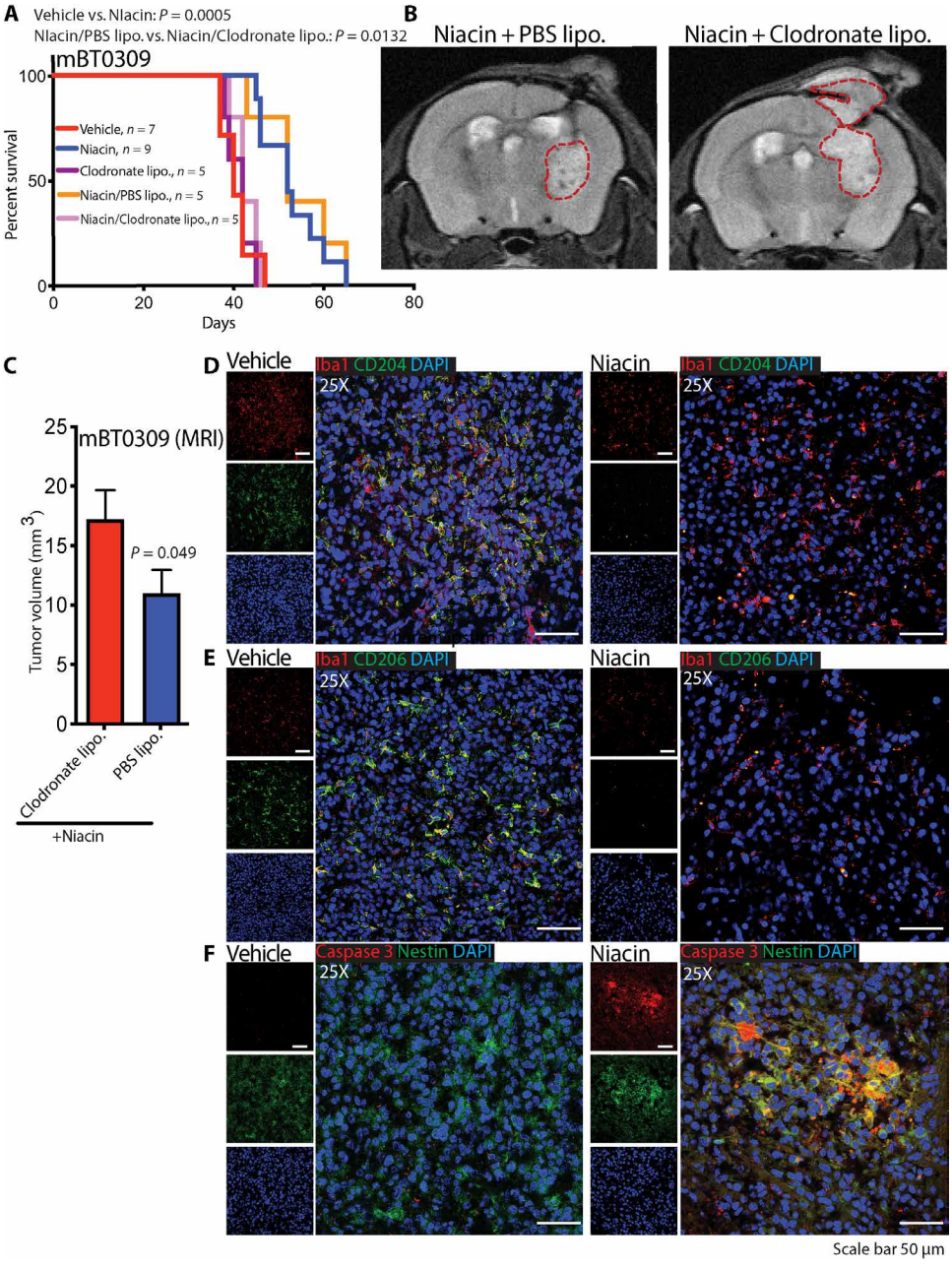

Fig. 5. Therapeutic efficacy of niacin requires myeloid cells in immunocompetent mice with syngeneic mBT0309 implants. (**A**) Kaplan-Meier analysis of niacin on survival ($P = 0.005$, log-rank test) in animals treated with niacin and/or clodronate liposomes. (**B** and **C**) MRI images (B) of niacin-treated mice depleted of monocytes by clodronate liposomes in C57BL/6 mice with syngeneic mBT0309 implants ($n = 5$ to 10 per group), and quantitation (C) of tumor volume from MRI images (unpaired *t* test). In this figure, the MRI images were acquired using a less sensitive MRI owing to breakdown of the preferred magnet, so the tumor on MRI is outlined in red. (**D** and **E**) Immunohistochemical analysis of brain tumor sections to detect anti-inflammatory $CD204^+$ (D) and $CD206^+$ (E) $Iba1^+$ macrophages/microglia. (**F**) Cleaved caspase 3 to detect apoptotic cells within the tumor in mouse brain sections.

knocked out in clones 8-1E12 and 8-1G12 (designated as *Ifnar1* KO 8-1E12 and 8-1G12) mouse BTIC cells (fig. S12). The effect of IFN-α14 on IFN-responsive genes was completely abrogated in *Ifnar1* KO mouse BTIC cells in vitro (Fig. 6A). Moreover, whereas recombinant murine pan IFN-α (mIFN-α) or mouse IFN-α14 (mIFN-α14) reduced the growth of wild-type (WT) BTICs, this effect was completely abrogated in the *Ifnar1* KO (8-1E12 and 8-1G12) mouse BTIC cells (Fig. 6, B and C). Notably, the conditioned medium from niacin-treated mouse BMDMs (Niacin-MøCM) could no longer reduce BTIC growth in *Ifnar1* KO (8-1E12 and 8-1G12) mouse BTIC cells, unlike the case for WT cells (Fig. 6, D and E).

To corroborate the in vitro results, we implanted *Ifnar1 KO* (8-1G12) or WT cells in syngeneic immunocompetent C57BL/6 mice and started treatment with niacin or vehicle 7 days after. The therapeutic efficacy of niacin was recapitulated in mice with WT BTICs, as evidenced through extended survival. In contrast, the therapeutic benefit of niacin no longer manifested in mice implanted with *Ifnar1* KO BTIC cells (Fig. 6F). This result implicates type 1 IFN signaling as one of the crucial mediators involved in niacin-mediated BTIC growth reduction.

Combination therapy with niacin and temozolomide further enhances longevity of mice with intracranial BTICs

We determined whether temozolomide, a U.S. Food and Drug Administration–approved alkylating chemotherapeutic drug used in GBM, could add to the therapeutic effects of niacin in reducing BTIC growth by mobilizing myeloid cells. Whereas temozolomide (100 μM) and Niacin-MonoCM by themselves reduced BTIC growth in culture, the most marked decrease of growth occurred when these were combined (fig. S13).

Next, we addressed whether niacin and temozolomide have combinatorial effects in mice implanted with intracranial patient-derived BTICs. We used BT048 and BT53M, which are both MGMT methylated and temozolomide sensitive (*22*). For the mice with BT048 implants, temozolomide (40 mg/kg) was given orally 5 days/week for 3 consecutive weeks with a break of 2 days of no injection between weeks. This was unexpectedly toxic, resulting in six deaths in the first week of temozolomide treatment, and the mice that died were excluded from analyses. For the remaining mice, MRI detection at day 49 showed a reduction in tumor volume in the niacin but not temozolomide or combination groups (Fig. 7A). Niacin and the combination treatment prolonged survival compared to vehicle based on Kaplan-Meier analysis (Fig. 7B), but the combination was not substantially different when compared to niacin. MRI analyses at day 49 in asymptomatic

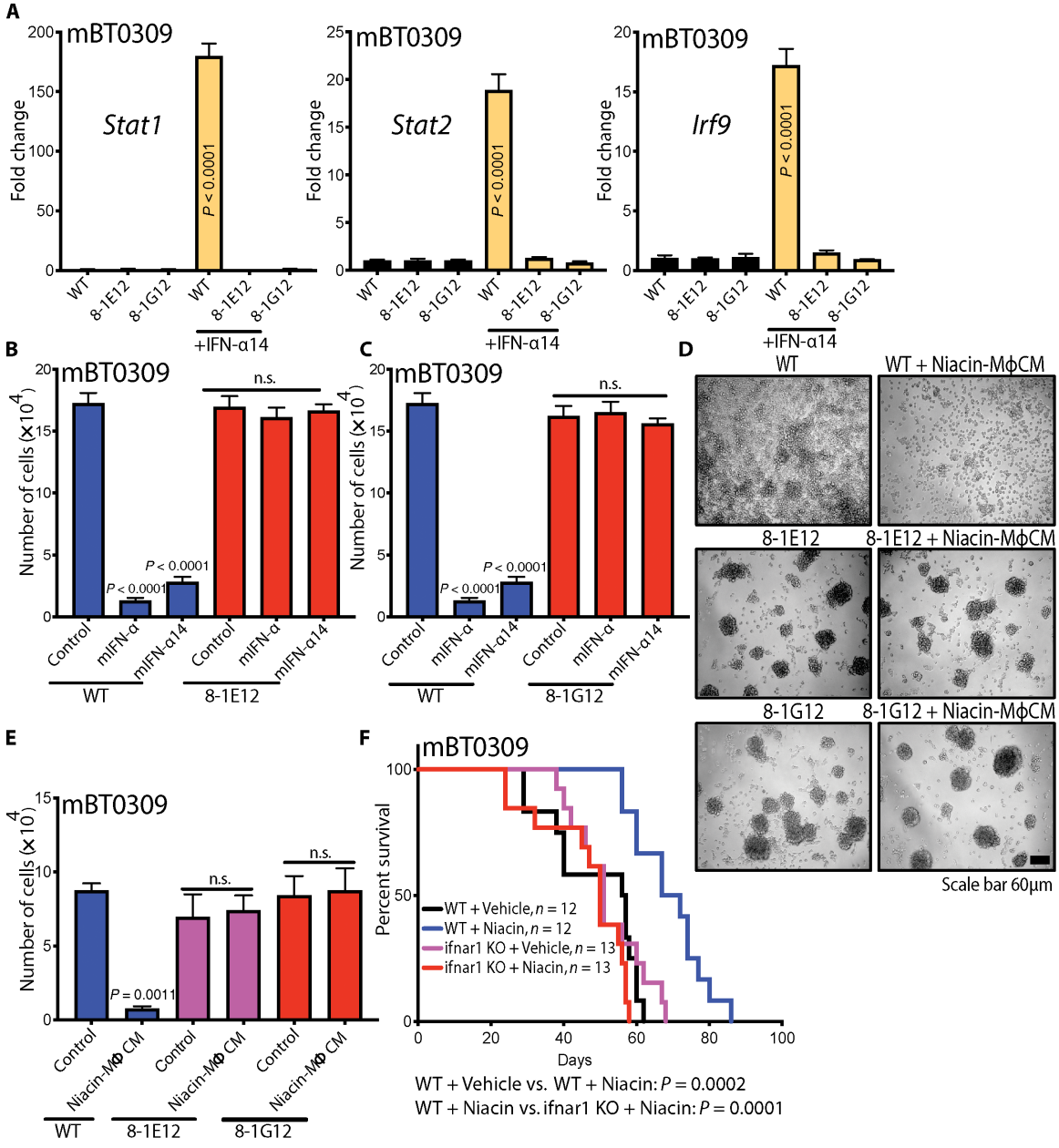

Fig. 6. Therapeutic efficacy of niacin is abrogated in mice harboring *Ifnar1* KO BTIC implants. IFNAR1 KO mouse BTIC cells were generated using CRISPR gene editing (fig. S12). (**A**) WT mBT0309 cells were treated with murine IFN-α14, and the expression of IFN-responsive genes *Stat1*, *Stat2*, and *Irf9* was determined. Similarly, *Stat1*, *Stat2*, and *Irf9* expression was determined in *Ifnar1 KO* (8-1E12 and 8-1G12) cells upon treatment with IFN-α14; one-way ANOVA compared to WT BTICs. (**B** and **C**) Effects of recombinant mIFN-α or mIFN-α14 on WT mBT0309 and *Ifnar1 KO* 8-1E12 (B) and 8-1G12 (C) murine cells (one-way ANOVA compared to control). (**D** and **E**) Effect of niacin-treated macrophage conditioned medium (Niacin-MØCM) on WT and *Ifnar1 KO* BTIC cells, showing representative images (D) (scale bar represents 60 μm) and quantification (E). All bars are means ± SEM of quadruplicate cultures and analyzed by one-way ANOVA. (**F**) Survival benefit with niacin was determined with Kaplan-Meier analysis in WT or *Ifnar1* KO (8-1G12) implanted mice (log-rank test). n.s., not significant.

animals showed smaller tumors in niacin or combination treatment mice compared to vehicle or temozolomide animals (Fig. 7C). A single survivor in the niacin plus temozolomide group of BT048-implanted mice receiving daily niacin treatment died after a year, indicating a marked increase in survival.

We repeated the niacin/temozolomide experiment in mice implanted with the BT53M line, where we reduced the temozolomide dose to 30 mg/kg and adjusted its interval (gap of 1 week of no treatment with temozolomide between the second and third week) to minimize its toxicity. MRI was conducted on day 36, when one vehicle-treated mouse was manifesting signs of tumor-associated toxicity (lethargy, fluffed fur). Figure 7D shows that whereas vehicle-treated mice already had measurable tumor volume, no MRI-detectable tumor was found in the other three groups at this early time point. Subsequent survival analyses show that temozolomide improved survival, which was exceeded in the niacin group. Notably, the combination of

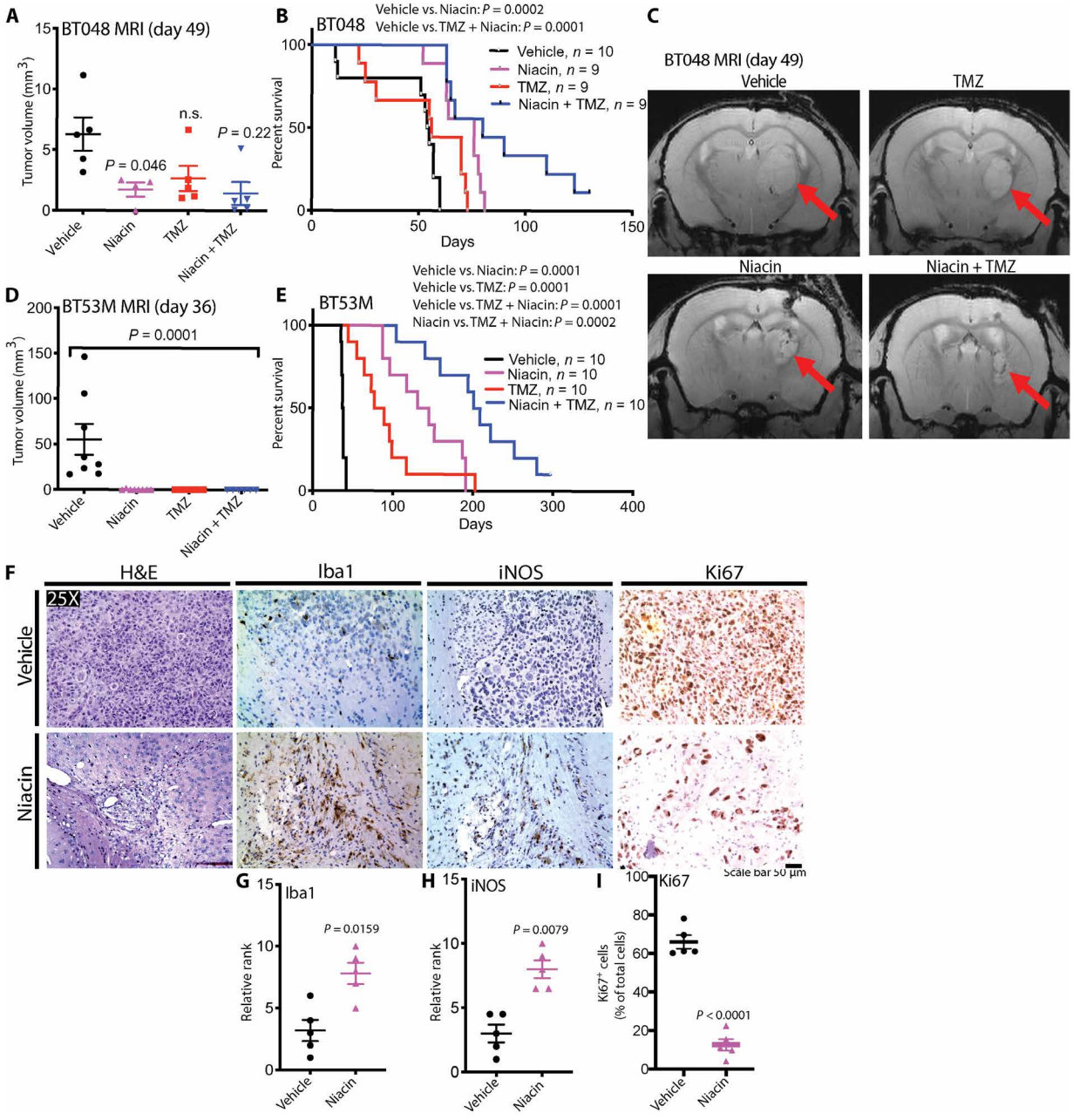

Fig. 7. Temozolomide promotes the life-extending efficacy of niacin in mice with GBM patient–derived BTICs. (**A** to **C**) SCID mice were implanted with BT048 cells and initiated on treatment 7 days later with daily niacin (100 mg/kg, >>>intraperitoneally), temozolomide (TMZ; oral, 40 mg/kg per dose in ORA-Plus for a round of 5 days/week for three consecutive weeks), the combination of niacin plus temozolomide as per the individual dose schedule, or vehicle (intraperitoneal saline and oral ORA-Plus). MRI was done at day 49 and quantified (A; *P* value relative to vehicle, one-way ANOVA with Tukey's post hoc test). Kaplan-Meier analysis to assess the therapeutic benefit of niacin and/or temozolomide (log-rank Mantel-Cox test) is displayed in (B). (C) Representative MRI images with arrows pointing to tumor. (**D** and **E**) In mice implanted with BT53M, the same four treatments as in (A) to (C) were used, except that the temozolomide dose was reduced to 30 mg/kg, and there was a gap of 1 week of no treatment with temozolomide between the second and third week. Temozolomide was no longer given after the third round of weekly administration. (D) Imaging was performed at day 36, and MRI-detected tumor was found only in the vehicle group. (E) Kaplan-Meier analysis to assess the therapeutic benefit of niacin and/or temozolomide (log-rank Mantel-Cox test). (**F**) A subset of the BT53M mice treated with vehicle or niacin were sacrificed at day 30 for histology; the tumor in the vehicle group manifested as a high density of cells detected by hematoxylin and eosin (H&E) staining. Tumor sections were also stained for Iba1, iNOS as a marker of proinflammatory macrophages/microglia, and Ki67 as a marker of proliferation. (**G** to **I**) Quantitation of Iba1-positive (G), iNOS-positive (H), and Ki67-positive (I) cells (Mann-Whitney *U* test).

niacin and temozolomide markedly prolonged survival by at least fivefold compared to vehicle-treated mice; the combination also conferred a survival advantage ($P = 0.002$) when compared to niacin (Fig. 7E).

We repeated the BT53M implants in a different experiment for histology comparisons, focusing on vehicle and niacin treatment. In this second experiment, where 7000 instead of the usual 10,000 BT53M cells were implanted, asymptomatic mice were euthanized

at 7 weeks after implantation. Tumors detected by hematoxylin and eosin staining in vehicle mice were larger (covering the entire field in Fig. 7F) when compared to those in niacin-treated animals (tumor was confined to the center of the field). Iba1 and iNOS (inducible nitric oxide synthase) staining, indicative of a proinflammatory macrophage/microglia population (Fig. 7F), were more evident in the niacin-treated group and corroborated by blinded rank-order analyses (Fig. 7, G and H). Moreover, the tumors in the vehicle-treated mice showed a higher proliferation index, as detected by Ki67 staining, compared to those in niacin-treated animals (Fig. 7, F and I). Overall, these results affirm the efficacy of niacin in reducing tumor volume, prolonging survival, and adding to the therapeutic effect of temozolomide.

The inefficient monocytes from GBM patients are reactivated by niacin to reduce BTIC growth in culture

Unlike cells from healthy human volunteers, monocytes isolated from the blood of four GBM patients did not inhibit the growth of allogeneic human BTICs (Fig. 8, A to D). Notably, niacin increased IFN-α14 in all four GBM-derived MonoCM (Fig. 8E) and restored their capacity to reduce BTIC sphere formation (Fig. 8, A to D). When IFNAR1 was reduced by siRNA in BTICs, niacin no longer reactivated the tumor growth–inhibiting capacity of GBM patient–derived monocytes (Fig. 8, F and G), thus supporting the involvement of IFN-α14 in niacin-induced tumor control. Notably, when monocytes derived from one of these patients with GBM were treated with niacin ex vivo, they exhibited proinflammatory phenotypes, as evidenced by increases in TNF-α, IL-1β, MIP-1β (CCL4), and RANTES (CCL5) proteins (fig. S14). These patient-derived cells did not require priming with LPS for cytokine elevation, in contrast to that noted for cells from normal individuals (Fig. 1).

DISCUSSION

We previously reported that macrophages/microglia from healthy individuals curb BTIC growth in culture, but that this property is lost in cells from patients with GBM (*22*). Our current work proposes niacin treatment as a means to overcome the compromised immunity. Although niacin is believed to have anti-inflammatory properties (*36*, *37*), our results demonstrate that niacin stimulated proinflammatory properties in vitro when used at pharmacologically relevant concentrations. We discovered that some features of niacin, such as proinflammatory cytokine elevation, require a priming stimulus in most cases, whereas others including phagocytosis, transcriptomic changes, and elevation of some chemokines do not. For example, an increase in CCL3 and CCL4 chemokines was observed upon niacin exposure in the absence of any priming stimulus. Of interest, CCL3 has been reported to confer antitumor properties in cancers such as melanoma (*54*, *55*). Notably, we found that conditioned medium collected from monocytes exposed to niacin without a priming stimulus decreased sphere formation in all nine genetically diverse BTIC lines regardless of MGMT status. BTIC growth inhibition induced by niacin-exposed monocytes resulted from reduced cell cycling, induction of apoptosis, and reduced stemness.

The potent growth-reducing effect of niacin-treated monocytes on BTICs provided impetus to evaluate its therapeutic efficacy in vivo. In mice with intracranial syngeneic or GBM patient–derived BTIC implants, treatment with niacin reduced tumor volume, as detected through MRI and histology, and prolonged the life span of tumor-bearing mice. In this regard, it is important to note that all niacin-treated mice had established tumor, and they all eventually died despite the marked survival benefits; this includes the lone niacin survivor in Fig. 7E that eventually died after the experiment was terminated and in which the presence of tumor was verified at autopsy.

The key role of myeloid cells as intermediaries of the niacin benefit was demonstrated by the decreased signal in ferumoxytol MRI and by the loss of niacin efficacy in mice depleted of circulating monocytes. These myeloid cells appeared to take on a more proinflammatory phenotype, as suggested by the increased number of proinflammatory iNOS-positive, and the reduced number of anti-inflammatory CD204/206-positive, Iba1 cells within tumors. Niacin treatment reduced growth of tumor in mice, as evidenced by reduced Ki67 proliferation index and positive staining for cleaved caspase 3, indicative of apoptosis.

With regard to whether myeloid polarization by niacin is required for the overall antitumor activity of niacin, it would be instructive to perform an experiment where niacin is given to mice in which the proinflammatory switch is prevented. Such an experiment is challenging to conduct because many triggers and signaling cascades affect myeloid polarization and they cannot all be antagonized.

Our experiments do not discriminate which myeloid cell population is the principal target of niacin activity, but the easier access of circulating monocytes to niacin, as well as their depletion by clodronate liposomes, would suggest that circulating monocytes are a key target. Notably, the combination of niacin and the current drug standard of care, temozolomide, showed an even better survival benefit than either agent alone, highlighting the potential of adding niacin to the current therapeutic regimen for GBM. This is supported by the capacity of niacin to reactivate the BTIC growth inhibitory ability of GBM patient–derived monocytes; such a bioassay may be used in the future to monitor responsiveness to niacin therapy.

In the majority of our studies, BTICs were exposed to the conditioned medium of niacin-stimulated myeloid cells, as these were growing from singly dissociated cells. Nonetheless, Niacin-MonoCM was also effective against well-established tumor spheres, where it disintegrated the spheres and prevented their further growth. This is encouraging for the use of niacin in GBM, especially because niacin would likely be initiated on top of standard therapy after the resection of bulk tumor in patients with GBM.

A recent article reported that niacin inhibits the assembly of the leading edge of U251 GBM line cells in culture (*56*). However, these authors used concentrations in the range of 3.5 to 7 mM, which are unlikely to be encountered in vivo. As noted earlier, in humans taking 1 g of niacin for dyslipidemia, the mean range of niacin detected in serum was 120 to 230 μM between 1 to 2 hours after intake (*34*).

We implicate IFN-α14 as a molecule secreted by niacin-treated myeloid cells to reduce BTIC growth, given that this is the only type 1 IFN increased in the microarray analyses of niacin-exposed monocytes, its protein content increases in the conditioned medium of niacin-stimulated monocytes, and the treatment of BTICs with siRNA to IFNAR1 abrogated the growth inhibitory efficacy of Niacin-MonoCM from control or GBM patients. Furthermore, Niacin-MøCM could not attenuate the growth of *Ifnar1* KO mouse BTIC cells in culture. Moreover, in mice with intracerebral grafts of BTICs that were devoid of IFNAR1, niacin was no longer efficacious. However, the amounts of basal and niacin-stimulated IFN-α14 were comparable in the conditioned medium of monocytes from control or GBM patients, suggesting that other factors are at play and that the

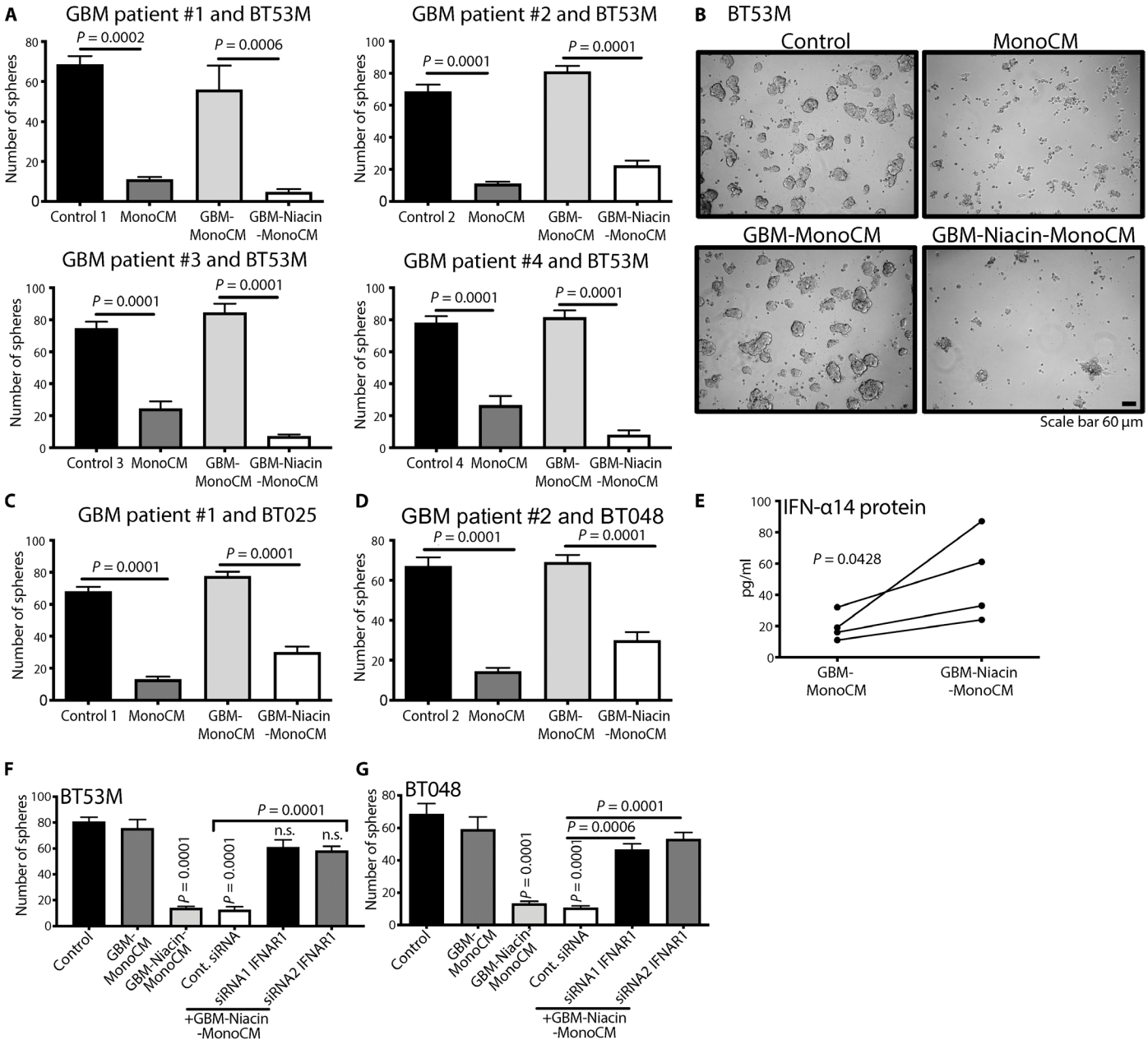

Fig. 8. Monocytes from patients with GBM do not suppress BTIC growth in culture, but are reactivated by ex vivo exposure to niacin. (**A**) Blood-derived monocytes were cultured from four patients with GBM peri-operatively, and samples of conditioned medium were obtained. BT53M cells were then exposed to conditioned medium of monocytes from healthy volunteers (MonoCM) or to conditioned medium from GBM-derived monocytes without (GBM-MonoCM) or with previous niacin (100 μM) treatment (GBM-Niacin-MonoCM); sphere formation was evaluated. (**B**) Representative images of the BT53M cells after 2 days; scale bar, 60 μm. (**C** and **D**) MonoCM or Niacin-MonoCM from GBM patients 1 (C) and 2 (D) were also tested on BT025 and BT048 lines for sphere formation. (**E**) IFN-α14 protein concentration in the conditioned medium of monocytes from four patients with GBM under basal conditions or niacin stimulation (paired *t* test, each line represents a single patient). (**F** and **G**) The capacity of GBM-Niacin-MonoCM to reduce BTIC growth was also determined in siRNA IFNAR1 knockdown of BT53M (F) and BT048 (G) cells. All bars are means ± SEM of quadruplicate cultures and analyzed by one-way ANOVA with Tukey's multiple comparisons post hoc test; *P* values are for comparisons against GBM-MonoCM unless otherwise indicated.

activity of IFN-α14 in GBM-derived monocytes is blocked until stimulation by niacin.

We note that IFN-α14 (20 to 150 pg/ml) was detected in the conditioned medium of niacin-stimulated monocytes, whereas recombinant IFN-α14 (5 to 100 ng/ml) was needed to reduce BTIC growth. This is likely because cells in culture are producing IFN-α14 into a relatively large volume of conditioned medium, so the amount measured reflects a dilution of the target protein. In other studies, cytokines were measured at much lower concentrations than those required to elicit a response in culture (*57*). We attempted to measure IFN-α14 in the serum of mice treated with niacin, but the amount was below the limit of detection in treated and control mice.

The molecular mechanism of niacin-induced IFN-α14 expression or of IFN-α14–induced cell cycle arrest and apoptosis of BTICs is currently not known. However, type I IFNs regulate the transcription of a large number of downstream targets that have direct effects on tumor cells and contribute indirectly through immune effector cells to contain tumors (*58*–*60*). Consistent with these reports, our study identified transcriptional induction of IFN-stimulated genes upon treatment with recombinant IFN-α14 in BTIC cells, such as *STAT1*, *STAT2*, and *IRF9*, which were increased in the PCR array.

In interrogating three separate GBM databases (GEO accession numbers GSE4536 and GSE7696, and TCGA), we found no abnormalities of IFN-α14 or niacin signaling in GBM. Given the low amount of *IFNA14* transcript, we were not able to determine its associations with specific immune cell signatures in the TCGA database, including those of tumor-associated macrophages, regulatory T cells, myeloid-derived suppressor cells, and effector T cells. These observations do not preclude the pharmacological use of niacin to mobilize myeloid cells to inhibit BTICs in GBM, as our results show.

There are several shortcomings to our study. Besides the inability to prove unequivocally that the switch of macrophages/microglia to a proinflammatory phenotype is a prerequisite for niacin efficacy in vivo, we initiated niacin at 7 days after implantation of BTICs in mice, a time point when tumor should not yet be fully established in the brain. Future experiments should initiate niacin treatment at later time points when tumors are larger, although we note that a GBM patient would normally undergo surgery to remove any detectable tumor mass before the initiation of chemotherapeutics. Another shortcoming is our use of the intraperitoneal route of administration of niacin, whereas this is taken as an oral medication in humans. We used the intraperitoneal route as proof of principle because absorption by this route is more reliable than by oral gavage or the use of drug in the drinking water. In addition, because of the much smaller size of tumors in niacin-treated mice, we were unable to ascertain with confidence whether the density of angiogenesis was reduced by its treatment. Last, it would be of interest to administer niacin along with radiation therapy that patients are subjected to standard of care in GBM or with checkpoint inhibitors, and these are future experiments that should be conducted.

In conclusion, we propose the immune-stimulatory activity of niacin, a common vitamin that could be rapidly translated into clinical use, as an adjunctive treatment for patients with GBM. The subverted myeloid immunity in other cancers could also be conducive for niacin intervention, but this remains to be determined in future studies.

MATERIALS AND METHODS

Study design

We determined sample sizes in the in vivo mouse model of tumor development based on our previous experience (*22*, *40*). We commonly used 9 to 10 mice per group to determine the therapeutic efficacy of niacin in the presence or absence of temozolomide because this was expected to sufficiently power the study to determine statistical significance. Because a principal objective of the animal experiments was to determine whether niacin prolonged the life of animals with intracranial BTICs, we used Kaplan-Meier survival curves, where mice found dead in their cages were recorded. In addition, in accordance with ethics guidelines, mice that were moribund (negligible limb movement or loss of 25% of body weight from the preceding few days) were considered to be at an end-point and immediately sacrificed. We also determined an outlier criterion for the vehicle-treated mice, that is, we excluded any vehicle-treated mice that did not develop tumor within 30 to 45 days after implantation as determined by MRI. We excluded any vehicle- or niacin-treated mice that did not show any sign of tumor growth at sacrifice at least 45 dpi (days post-innoculation). Each xenograft experiment was performed at least twice, using tumor lines generated from GBM patients with different genetic backgrounds. In the syngeneic model, the therapeutic effect of niacin was evaluated at least twice; this was also the case for syngeneic *Ifnar1* KO cells implanted in C57BL/6 mice. All mouse protocols were approved by the Animal Care Committee at the University of Calgary in accordance with research guidelines from the Canadian Council for Animal Care.

Several of the experiments were carried out in a blinded manner. For MRI evaluation of tumor-bearing mice treated with niacin or vehicle, we blinded the researchers to the animal groups before data acquisition. Rank order analysis was used to quantify the histological and immunohistochemical data for intracranial tumors, and this was conducted in a blinded manner. In the experiment to determine whether niacin-treated macrophage conditioned medium (Niacin-MØCM) could reduce WT BTIC growth and whether the effect of Niacin-MØCM would have an effect on *Ifnar1* KO cells, the researchers were blinded. We also adopted an exclusion criterion for generating MonoCM from control human subjects, where monocytes were isolated from the venous blood of healthy adult individuals who were not on any anti-inflammatory medications. Last, GBM patient–derived BTIC cell lines were routinely checked using identity matching with the original parental lines. All experiments with human cells were conducted with approval from the Conjoint Health Research Ethics Board, University of Calgary, with informed consent from the human subjects.

Animals, BTIC implantation, treatment, and monitoring

BTIC spheres from BT012, BT048, and BT53M lines or mouse mBT0309 spheres were mechanically dissociated into single-cell suspensions. Cells were washed with BTIC medium. Unless otherwise stated, 10,000 human or 25,000 murine cells were resuspended in 2 μl of PBS and implanted into the right striatum of 6- to 8-week-old female SCID or C57BL/6 mice (Charles River) stereotactically (*22*). Seven days after implantation, mice were treated with niacin at a dose of 100 mg/kg daily (intraperitoneally) until the termination of the experiment. Control mice were injected with an identical vehicle (saline) solution.

In another series of experiments, mice were treated with a combination of niacin and temozolomide. Both niacin and temozolomide treatment were begun 7 days after implantation of BT048 cells, where niacin (100 mg/kg, intraperitoneally) was administered daily, whereas temozolomide (diluted in ORA-Plus) was given by oral gavage at a dose of 40 mg/kg of body weight for a round of 5 days/week for 3 weeks. In the second series of experiments involving BT53M, the dose of temozolomide was reduced to 30 mg/kg, and there was a gap of 1 week of no treatment with temozolomide between the second and third week. Temozolomide was no longer given after the third round of weekly administration. Vehicle-treated mice were administered intraperitoneal saline and ORA-Plus by gavage in the same schedule as the individual treatments.

To deplete monocytes/macrophages, we used clodronate liposomes (*22*). After implantation of BT048, BT053M, or syngeneic mouse BT0309 cells, mice were treated intravenously via the tail vein with

liposomes at day 7 after implantation with 200 μl of either control PBS– or clodronate-containing liposomes once per week for the duration of the niacin treatment.

Statistical analyses

Kaplan-Meier survival curves were analyzed for statistical differences between groups using the log-rank Mantel-Cox test. For analyses of differences in experiments involving multiple groups, but where comparisons were made to a single group (such as to LPS in Fig. 1), a one-way analysis of variance (ANOVA) with Dunnett's post hoc test was used. For multiple group comparisons to controls or to other subgroups within the same experiment, a one-way ANOVA with Tukey's post hoc comparisons was used. For analyses of parametric data between two groups, we used an unpaired *t* test (two-tailed unless otherwise stated). For analyses of nonparametric data between two groups, a Mann-Whitney *U* test was used. Original data are in data file S3.

SUPPLEMENTARY MATERIALS

stm.sciencemag.org/cgi/content/full/12/537/eaay9924/DC1
Materials and Methods
Fig. S1. Characteristics of BMDMs.
Fig. S2. Effects of niacin in mouse macrophages and human monocytes: Cytokines, chemokines, and arginase activity.
Fig. S3. Niacin does not affect the viability or differentiation of monocytes.
Fig. S4. Reduction of BTIC growth by the conditioned medium of niacin-stimulated monocytes.
Fig. S5. Effects of Niacin-MonoCM or IFN-α14 on BTIC growth, cell cycle progression, apoptosis, and stemness.
Fig. S6. Effects of Niacin-MonoCM, niacin, and IFN-α14 on BTICs.
Fig. S7. Effect of mouse IFN-α14 on BT53M cells.
Fig. S8. IFN-α14 gene (*IFNA14*) expression and association with survival in GBM.
Fig. S9. TCGA analysis of other soluble factors.
Fig. S10. Clodronate liposome treatment depletes monocytes/macrophages as visualized by spinning-disc confocal microscopy of the liver.
Fig. S11. Peripheral and CNS infiltrating T lymphocytes in mice treated with niacin.
Fig. S12. Confirmation of mouse *Ifnar1* gene KO by DNA sequencing.
Fig. S13. Effects of Niacin-MonoCM and temozolomide on BT048 growth in culture.
Fig. S14. Analysis of GBM patient–derived monocytes upon niacin stimulation.
Data file S1. Differential gene expression in human monocytes upon niacin treatment (raw data).
Data file S2. Human Interferon Pathway TaqMan Array of human BTIC lines upon treatment with IFN-α14.
Data file S3. Raw data from experiments reported in composite figures.
References (*61*, *62*)

View/request a protocol for this paper from *Bio-protocol*.

REFERENCES AND NOTES

1. R. Stupp, W. P. Mason, M. J. van den Bent, M. Weller, B. Fisher, M. J. Taphoorn, K. Belanger, A. A. Brandes, C. Marosi, U. Bogdahn, J. Curschmann, R. C. Janzer, S. K. Ludwin, T. Gorlia, A. Allgeier, D. Lacombe, J. G. Cairncross, E. Eisenhauer, R. O. Mirimanoff; European Organisation for Research and Treatment of Cancer Brain Tumor and Radiotherapy Groups; National Cancer Institute of Canada Clinical Trials Group, Radiotherapy plus concomitant and adjuvant temozolomide for glioblastoma. *N. Engl. J. Med.* **352**, 987–996 (2005).
2. J. Chen, Y. Li, T.-S. Yu, R. M. McKay, D. K. Burns, S. G. Kernie, L. F. Parada, A restricted cell population propagates glioblastoma growth after chemotherapy. *Nature* **488**, 522–526 (2012).
3. J. D. Lathia, J. M. Heddleston, M. Venere, J. N. Rich, Deadly teamwork: Neural cancer stem cells and the tumor microenvironment. *Cell Stem Cell* **8**, 482–485 (2011).
4. N. A. Charles, E. C. Holland, R. Gilbertson, R. Glass, H. Kettenmann, The brain tumor microenvironment. *Glia* **60**, 502–514 (2012).
5. C. C. Poon, S. Sarkar, V. W. Yong, J. J. P. Kelly, Glioblastoma-associated microglia and macrophages: Targets for therapies to improve prognosis. *Brain* **140**, 1548–1560 (2017).
6. R. Mirzaei, S. Sarkar, V. W. Yong, T cell exhaustion in glioblastoma: Intricacies of immune checkpoints. *Trends Immunol.* **38**, 104–115 (2017).
7. B. Zhang, R. Shen, S. Cheng, L. Feng, Immune microenvironments differ in immune characteristics and outcome of glioblastoma multiforme. *Cancer Med.* **8**, 2897–2907 (2019).
8. A. Dirkse, A. Golebiewska, T. Buder, P. V. Nazarov, A. Muller, S. Poovathingal, N. H. C. Brons, S. Leite, N. Sauvageot, D. Sarkisjan, M. Seyfrid, S. Fritah, D. Stieber, A. Michelucci, F. Hertel, C. Herold-Mende, F. Azuaje, A. Skupin, R. Bjerkvig, A. Deutsch, A. Voss-Böhme, S. P. Niclou, Stem cell-associated heterogeneity in Glioblastoma results from intrinsic tumor plasticity shaped by the microenvironment. *Nat. Commun.* **10**, 1787 (2019).
9. W. Tomaszewski, L. Sanchez-Perez, T. F. Gajewski, J. H. Sampson, Brain tumor microenvironment and host state: Implications for immunotherapy. *Clin. Cancer Res.* **25**, 4202–4210 (2019).
10. C. C. Poon, P. M. K. Gordon, K. Liu, R. Yang, S. Sarkar, R. Mirzaei, S. T. Ahmad, M. L. Hughes, V. W. Yong, J. J. P. Kelly, Differential microglia and macrophage profiles in human IDH-mutant and -wild type glioblastoma. *Oncotarget* **10**, 3129–3143 (2019).
11. S. Sarkar, C. C. Poon, R. Mirzaei, K. S. Rawji, W. Hader, P. Bose, J. Kelly, J. F. Dunn, V. W. Yong, Microglia induces Gas1 expression in human brain tumor-initiating cells to reduce tumorigenecity. *Sci. Rep.* **8**, 15286 (2018).
12. M. C. Takenaka, G. Gabriely, V. Rothhammer, I. D. Mascanfroni, M. A. Wheeler, C.-C. Chao, C. Gutiérrez-Vázquez, J. Kenison, E. C. Tjon, A. Barroso, T. Vandeventer, K. A. de Lima, S. Rothweiler, L. Mayo, S. Ghannam, S. Zandee, L. Healy, D. Sherr, M. F. Farez, A. Prat, J. Antel, D. A. Reardon, H. Zhang, S. C. Robson, G. Getz, H. L. Weiner, F. J. Quintana, Control of tumor-associated macrophages and T cells in glioblastoma via AHR and CD39. *Nat. Neurosci.* **22**, 729–740 (2019).
13. K. Gabrusiewicz, X. Li, J. Wei, Y. Hashimoto, A. L. Marisetty, M. Ott, F. Wang, D. Hawke, J. Yu, L. M. Healy, A. Hossain, J. C. Akers, S. N. Maiti, S. Yamashita, Y. Shimizu, K. Dunner, M. A. Zal, J. K. Burks, J. Gumin, F. Nwajei, A. Rezavanian, S. Zhou, G. Rao, R. Sawaya, G. N. Fuller, J. T. Huse, J. P. Antel, S. Li, L. Cooper, E. P. Sulman, C. Chen, C. Geula, R. Kalluri, T. Zal, A. B. Heimberger, Glioblastoma stem cell-derived exosomes induce M2 macrophages and PD-L1 expression on human monocytes. *Oncoimmunology* **7**, e1412909 (2018).
14. S. M. Pyonteck, L. Akkari, A. J. Schuhmacher, R. L. Bowman, L. Sevenich, D. F. Quail, O. C. Olson, M. L. Quick, J. T. Huse, V. Teijeiro, M. Setty, C. S. Leslie, Y. Oei, A. Pedraza, J. Zhang, C. W. Brennan, J. C. Sutton, E. C. Holland, D. Daniel, J. A. Joyce, CSF-1R inhibition alters macrophage polarization and blocks glioma progression. *Nat. Med.* **19**, 1264–1272 (2013).
15. D. F. Quail, R. L. Bowman, L. Akkari, M. L. Quick, A. J. Schuhmacher, J. T. Huse, E. C. Holland, J. C. Sutton, J. A. Joyce, The tumor microenvironment underlies acquired resistance to CSF-1R inhibition in gliomas. *Science* **352**, aad3018 (2016).
16. J. Held-Feindt, K. Hattermann, S. S. Müerköster, H. Wedderkopp, F. Knerlich-Lukoschus, H. Ungefroren, H. M. Mehdorn, R. Mentlein, CX3CR1 promotes recruitment of human glioma-infiltrating microglia/macrophages (GIMs). *Exp. Cell Res.* **316**, 1553–1566 (2010).
17. W. Zhou, S. Q. Ke, Z. Huang, W. Flavahan, X. Fang, J. Paul, L. Wu, A. E. Sloan, R. E. McLendon, X. Li, J. N. Rich, S. Bao, Periostin secreted by glioblastoma stem cells recruits M2 tumour-associated macrophages and promotes malignant growth. *Nat. Cell Biol.* **17**, 170–182 (2015).
18. J. Wei, A. Marisetty, B. Schrand, K. Gabrusiewicz, Y. Hashimoto, M. Ott, Z. Grami, L.-Y. Kong, X. Ling, H. Caruso, S. Zhou, Y. A. Wang, G. N. Fuller, J. Huse, E. Gilboa, N. Kang, X. Huang, R. Verhaak, S. Li, A. B. Heimberger, Osteopontin mediates glioblastoma-associated macrophage infiltration and is a potential therapeutic target. *J. Clin. Invest.* **129**, 137–149 (2019).
19. C. Wang, K. Li, T. Li, Z. Chen, Y. Wen, X. Liu, X. Jia, Y. Zhang, Y. Xu, M. Han, N. Komatsu, L. Zhao, X. Chen, Monocyte-mediated chemotherapy drug delivery in glioblastoma. *Nanomedicine* **13**, 157–178 (2018).
20. P. Peixoto, A. Blomme, B. Costanza, R. Ronca, S. Rezzola, A. P. Palacios, L. Schoysman, S. Boutry, N. Goffart, O. Peulen, P. Maris, E. Di Valentin, V. Hennequière, E. Bianchi, A. Henry, P. Meunier, B. Rogister, R. N. Muller, P. Delvenne, A. Bellahcène, V. Castronovo, A. Turtoi, HDAC7 inhibition resets STAT3 tumorigenic activity in human glioblastoma independently of EGFR and PTEN: New opportunities for selected targeted therapies. *Oncogene* **35**, 4481–4494 (2016).
21. T. Kees, J. Lohr, J. Noack, R. Mora, G. Gdynia, G. Tödt, A. Ernst, B. Radlwimmer, C. S. Falk, C. Herold-Mende, A. Régnier-Vigouroux, Microglia isolated from patients with glioma gain antitumor activities on poly (I:C) stimulation. *Neuro Oncol.* **14**, 64–78 (2012).
22. S. Sarkar, A. Döring, F. J. Zemp, C. Silva, X. Lun, X. Wang, J. Kelly, W. Hader, M. Hamilton, P. Mercier, J. F. Dunn, D. Kinniburgh, N. van Rooijen, S. Robbins, P. Forsyth, G. Cairncross, S. Weiss, V. W. Yong, Therapeutic activation of macrophages and microglia to suppress brain tumor-initiating cells. *Nat. Neurosci.* **17**, 46–55 (2014).
23. L. Pang, Y. Zhu, J. Qin, W. Zhao, J. Wang, Primary M1 macrophages as multifunctional carrier combined with PLGA nanoparticle delivering anticancer drug for efficient glioma therapy. *Drug Deliv.* **25**, 1922–1931 (2018).
24. L. Lisi, E. Laudati, P. Navarra, C. Dello Russo, The mTOR kinase inhibitors polarize glioma-activated microglia to express a M1 phenotype. *J. Neuroinflammation* **11**, 125 (2014).
25. S. Mukherjee, A. Fried, R. Hussaini, R. White, J. Baidoo, S. Yalamanchi, P. Banerjee, Phytosomal curcumin causes natural killer cell-dependent repolarization of glioblastoma

(GBM) tumor-associated microglia/macrophages and elimination of GBM and GBM stem cells. *J. Exp. Clin. Cancer Res.* **37**, 168 (2018).
26. D. Saha, R. L. Martuza, S. D. Rabkin, Macrophage polarization contributes to glioblastoma eradication by combination immunovirotherapy and immune checkpoint blockade. *Cancer Cell* **32**, 253–267 e5 (2017).
27. J. Kloepper, L. Riedemann, Z. Amoozgar, G. Seano, K. Susek, V. Yu, N. Dalvie, R. L. Amelung, M. Datta, J. W. Song, V. Askoxylakis, J. W. Taylor, C. Lu-Emerson, A. Batista, N. D. Kirkpatrick, K. Jung, M. Snuderl, A. Muzikansky, K. G. Stubenrauch, O. Krieter, H. Wakimoto, L. Xu, L. L. Munn, D. G. Duda, D. Fukumura, T. T. Batchelor, R. K. Jain, Ang-2/VEGF bispecific antibody reprograms macrophages and resident microglia to anti-tumor phenotype and prolongs glioblastoma survival. *Proc. Natl. Acad. Sci. U.S.A.* **113**, 4476–4481 (2016).
28. S. Xu, J. Wei, F. Wang, L.-Y. Kong, X.-Y. Ling, E. Nduom, K. Gabrusiewicz, T. Doucette, Y. Yang, N. K. Yaghi, V. Fajt, J. M. Levine, W. Qiao, X.-G. Li, F. F. Lang, G. Rao, G. N. Fuller, G. A. Calin, A. B. Heimberger, Effect of miR-142-3p on the M2 macrophage and therapeutic efficacy against murine glioblastoma. *J. Natl. Cancer Inst.* **106**, dju162 (2014).
29. S. Samanani, M. Mishra, C. Silva, B. Verhaeghe, J. Wang, J. Tong, V. W. Yong, Screening for inhibitors of microglia to reduce neuroinflammation. *CNS Neurol. Disord. Drug Targets* **12**, 741–749 (2013).
30. J. C. Creider, R. A. Hegele, T. R. Joy, Niacin: Another look at an underutilized lipid-lowering medication. *Nat. Rev. Endocrinol.* **8**, 517–528 (2012).
31. W. E. Boden, M. S. Sidhu, P. P. Toth, The therapeutic role of niacin in dyslipidemia management. *J. Cardiovasc. Pharmacol. Ther.* **19**, 141–158 (2014).
32. M. K. Ito, Niacin-based therapy for dyslipidemia: Past evidence and future advances. *Am. J. Manag. Care* **8**, S315–S322 (2002).
33. A. Döring, S. Sloka, L. Lau, M. Mishra, J. van Minnen, X. Zhang, D. Kinniburgh, S. Rivest, V. W. Yong, Stimulation of monocytes, macrophages, and microglia by amphotericin B and macrophage colony-stimulating factor promotes remyelination. *J. Neurosci.* **35**, 1136–1148 (2015).
34. L. A. Carlson, L. Orö, J. Östman, Effect of a single dose of nicotinic acid on plasma lipids in patients with hyperlipoproteinemia. *Acta Med. Scand.* **183**, 457–465 (1968).
35. P. Perng, M. Lim, Immunosuppressive mechanisms of malignant gliomas: Parallels at non-CNS Sites. *Front. Oncol.* **5**, 153 (2015).
36. P. S. Lipszyc, G. A. Cremaschi, M. Zorrilla-Zubilete, M. L. Bertolino, F. Capani, A. M. Genaro, M. R. Wald, Niacin modulates pro-inflammatory cytokine secretion. A potential mechanism involved in its anti-atherosclerotic effect. *Open Cardiovasc. Med. J.* **7**, 90–98 (2013).
37. J. E. Digby, F. Martinez, A. Jefferson, N. Ruparelia, J. Chai, M. Wamil, D. R. Greaves, R. P. Choudhury, Anti-inflammatory effects of nicotinic acid in human monocytes are mediated by GPR109A dependent mechanisms. *Arterioscler. Thromb. Vasc. Biol.* **32**, 669–676 (2012).
38. C. Wakade, B. Giri, A. Malik, H. Khodadadi, J. C. Morgan, R. K. Chong, B. Baban, Niacin modulates macrophage polarization in Parkinson's disease. *J. Neuroimmunol.* **320**, 76–79 (2018).
39. A. Francke, J. Herold, S. Weinert, R. H. Strasser, R. C. Braun-Dullaeus, Generation of mature murine monocytes from heterogeneous bone marrow and description of their properties. *J. Histochem. Cytochem.* **59**, 813–825 (2011).
40. S. Sarkar, R. Mirzaei, F. J. Zemp, W. Wei, D. L. Senger, S. M. Robbins, V. W. Yong, Activation of NOTCH signaling by Tenascin-C promotes growth of human brain tumor-initiating cells. *Cancer Res.* **77**, 3231–3243 (2017).
41. X. Lun, J. C. Wells, N. Grinshtein, J. C. King, X. Hao, N.-H. Dang, X. Wang, A. Aman, D. Uehling, A. Datti, J. L. Wrana, J. C. Easaw, A. Luchman, S. Weiss, J. G. Cairncross, D. R. Kaplan, S. M. Robbins, D. L. Senger, Disulfiram when combined with Copper enhances the therapeutic effects of temozolomide for the treatment of glioblastoma. *Clin. Cancer Res.* **22**, 3860–3875 (2016).
42. M. D. Blough, D. C. Beauchamp, M. R. Westgate, J. J. Kelly, J. G. Cairncross, Effect of aberrant p53 function on temozolomide sensitivity of glioma cell lines and brain tumor initiating cells from glioblastoma. *J. Neuro Oncol.* **102**, 1–7 (2011).
43. M. D. Blough, M. R. Westgate, D. Beauchamp, J. J. Kelly, O. Stechishin, A. L. Ramirez, S. Weiss, J. G. Cairncross, Sensitivity to temozolomide in brain tumor initiating cells. *Neuro Oncol.* **12**, 756–760 (2010).
44. B. Davis, Y. Shen, C. C. Poon, H. A. Luchman, O. D. Stechishin, C. S. Pontifex, W. Wu, J. J. Kelly, M. D. Blough; Terry Fox Research Institute Glioblastoma Consortium, Comparative genomic and genetic analysis of glioblastoma-derived brain tumor-initiating cells and their parent tumors. *Neuro Oncol.* **18**, 350–360 (2016).
45. J. J. Kelly, O. Stechishin, A. Chojnacki, X. Lun, B. Sun, D. L. Senger, P. Forsyth, R. N. Auer, J. F. Dunn, J. G. Cairncross, I. F. Parney, S. Weiss, Proliferation of human glioblastoma stem cells occurs independently of exogenous mitogens. *Stem Cells* **27**, 1722–1733 (2009).
46. R. Spector, Niacin and niacinamide transport in the central nervous system. In vivo studies. *J. Neurochem.* **33**, 895–904 (1979).
47. L. V. Hankes, H. H. Coenen, E. Rota, K. J. Langen, H. Herzog, W. Wutz, G. Stoecklin, L. E. Feinendegen, Effect of Huntington's and Alzheimer's diseases on the transport of nicotinic acid or nicotinamide across the human blood-brain barrier. *Adv. Exp. Med. Biol.* **294**, 675–678 (1991).
48. J. N. Sarkaria, L. S. Hu, I. F. Parney, D. H. Pafundi, D. H. Brinkmann, N. N. Laack, C. Giannini, T. C. Burns, S. H. Kizilbash, J. K. Laramy, K. R. Swanson, T. J. Kaufmann, P. D. Brown, N. Y. R. Agar, E. Galanis, J. C. Buckner, W. F. Elmquist, Is the blood–brain barrier really disrupted in all glioblastomas? A critical assessment of existing clinical data. *Neuro Oncol.* **20**, 184–191 (2018).
49. T. Yamaoka, S. Kojima, S. Ichi, Y. Kashiwazaki, T. Koide, Y. Sokawa, Biologic and binding activities of IFN-alpha subtypes in ACHN human renal cell carcinoma cells and Daudi Burkitt's lymphoma cells. *J. Interferon Cytokine Res.* **19**, 1343–1349 (1999).
50. R. Yang, J. He, Y. Wang, Activation of the niacin receptor HCA_2 reduces demyelination and neurofilament loss, and promotes functional recovery after spinal cord injury in mice. *Eur. J. Pharmacol.* **791**, 124–136 (2016).
51. R. Yang, S. Sarkar, D. J. Korchinski, Y. Wu, V. W. Yong, J. F. Dunn, MRI monitoring of monocytes to detect immune stimulating treatment response in brain tumor. *Neuro Oncol.* **19**, 364–371 (2017).
52. M. M. Polfliet, P. H. Goede, E. M. van Kesteren-Hendrikx, N. van Rooijen, C. D. Dijkstra, T. K. van den Berg, A method for the selective depletion of perivascular and meningeal macrophages in the central nervous system. *J. Neuroimmunol.* **116**, 188–195 (2001).
53. A. Pisklakova, B. McKenzie, F. Zemp, X. Lun, R. S. Kenchappa, A. B. Etame, M. M. Rahman, K. Reilly, S. Pilon-Thomas, G. McFadden, E. Kurz, P. A. Forsyth, M011L-deficient oncolytic myxoma virus induces apoptosis in brain tumor-initiating cells and enhances survival in a novel immunocompetent mouse model of glioblastoma. *Neuro Oncol.* **18**, 1088–1098 (2016).
54. Y. Nakasone, M. Fujimoto, T. Matsushita, Y. Hamaguchi, D. L. Huu, M. Yanaba, S. Sato, K. Takehara, M. Hasegawa, Host-derived MCP-1 and MIP-1α regulate protective anti-tumor immunity to localized and metastatic B16 melanoma. *Am. J. Pathol.* **180**, 365–374 (2012).
55. A. Nakano, H. Yoneyama, S. Ueha, M. Kitabatake, S. Ishikawa, I. Kawase, H. Sugiyama, K. Matsushima, Intravenous administration of MIP-1alpha with intra-tumor injection of P. acnes shows potent anti-tumor effect. *Int. Immunopharmacol.* **7**, 845–857 (2007).
56. X. Yang, S. Mei, H. Niu, J. Li, Nicotinic acid impairs assembly of leading edge in glioma cells. *Oncol. Rep.* **38**, 829–836 (2017).
57. O. Dmitrieva-Posocco, A. Dzutsev, D. F. Posocco, V. Hou, W. Yuan, V. Thovarai, I. A. Mufazalov, M. Gunzer, I. P. Shilovskiy, M. R. Khaitov, G. Trinchieri, A. Waisman, S. I. Grivennikov, Cell-type-specific responses to interleukin-1 control microbial invasion and tumor-elicited inflammation in colorectal cancer. *Immunity* **50**, 166–180. e7 (2019).
58. E. C. Borden, Interferons α and β in cancer: Therapeutic opportunities from new insights. *Nat. Rev. Drug Discov.* **18**, 219–234 (2019).
59. D. Shen, C.-C. Guo, J. Wang, Z.-K. Qiu, K. Sai, Q.-Y. Yang, Y.-S. Chen, F.-R. Chen, J. Wang, L. Panasci, Z.-P. Chen, Interferon-α/β enhances temozolomide activity against MGMT-positive glioma stem-like cells. *Oncol. Rep.* **34**, 2715–2721 (2015).
60. W. Roth, B. Wagenknecht, J. Dichgans, M. Weller, Interferon-α enhances CD95L-induced apoptosis of human malignant glioma cells. *J. Neuroimmunol.* **87**, 121–129 (1998).
61. T. Montoya, M. L. Castejón, M. Sánchez-Hidalgo, A. González-Benjumea, J. G. Fernández-Bolaños, C. A. de-la-Lastra, Oleocanthal modulates LPS-induced murine peritoneal macrophages activation via regulation of inflammasome, Nrf-2/HO-1, and MAPKs signaling pathways. *J. Agric. Food Chem.* **67**, 5552–5559 (2019).
62. N. E. Reiner, Methods in molecular biology. Macrophages and dendritic cells. Methods and protocols. Preface. *Methods Mol. Biol.* **531**, v–vi (2009).

Acknowledgments: We acknowledge the technical help of J. Wang, C. Silva, F. Cavalcante Melo, Y. Fan, X. Wang, M. Kumar, and F. Yong. We thank the University of Calgary BTIC Core headed by S. Weiss and G. Cairncross for isolating BTIC lines from patient-resected specimens. We acknowledge the Microarray Facility at the Southern Alberta Cancer Research Institute (SACRI). We thank Y. Yu (Center for Genome Engineering, Cumming School of Medicine, University of Calgary) for the production of KO cell line using CRISPR technology. **Funding:** This work was supported by operating grants from Alberta Innovates—Health Solutions (AIHS) in collaboration with Alberta Cancer Foundation (V.W.Y., J.K., and J.F.D.), the Ronald and Irene Ward Foundation (V.W.Y.) and the Canadian Institutes of Health Research (V.W.Y.). MRI was supported, in part, with a Brain Canada platform grant (J.F.D.). K.R. was supported by a Vanier Canada Graduate Scholarship. R.M. was supported by a University of Calgary Eyes High postdoctoral scholarship. R.Y. acknowledges studentship support from AIHS and Branch Out Neurological Foundation. F.J.Z. was supported by AIHS, CIHR, and ACHRI postdoctoral scholarships. V.W.Y. is a Canada Research Chair (Tier 1) in Neuroimmunology for which salary support is gratefully acknowledged. **Author contributions:** S.S. performed and oversaw the majority of the experiments, wrote the first draft of the manuscript, and edited subsequent versions. R.Y. conducted the MRI experiments and edited the manuscript. R.M. contributed to FACS analysis, PCR array, and microarray data analysis, helping with constructing figures and

editing the manuscript. K.R. provided the data that niacin stimulates myeloid cells, and edited the manuscript. C.P. and M.K.M. contributed data and edited the manuscript. F.J.Z. conducted the brain implantation experiments and edited the manuscript. P.B. mined the GBM databases and edited the manuscript. J.K. and J.F.D. provided supervision and edited the manuscript. V.W.Y. supervised the entire study and finalized the manuscript. **Competing interests:** The authors declare that they have no competing interests. **Data and materials availability:** The microarray data have been deposited in the GEO depository, accession number GSE103381. All other data are provided in the main manuscript or the Supplementary Materials.

Submitted 3 August 2019
Accepted 9 March 2020
Published 1 April 2020
10.1126/scitranslmed.aay9924

Citation: S. Sarkar, R. Yang, R. Mirzaei, K. Rawji, C. Poon, M. K. Mishra, F. J. Zemp, P. Bose, J. Kelly, J. F. Dunn, V. W. Yong, Control of brain tumor growth by reactivating myeloid cells with niacin. *Sci. Transl. Med.* **12**, eaay9924 (2020).

Science Translational Medicine

Control of brain tumor growth by reactivating myeloid cells with niacin

Susobhan Sarkar, Runze Yang, Reza Mirzaei, Khalil Rawji, Candice Poon, Manoj K. Mishra, Franz J. Zemp, Pinaki Bose, John Kelly, Jeff F. Dunn and V. Wee Yong

Sci Transl Med **12**, eaay9924.
DOI: 10.1126/scitranslmed.aay9924

An old vitamin's new tricks

Although innate immune cells are typically present inside tumors, they often have an inactive phenotype such that they are ineffective at killing the cancer cells or even promote tumor growth. Sarkar *et al*. discovered that it may be possible to reprogram these cells to a more active type using niacin (vitamin B3). The authors showed that niacin-exposed monocytes can inhibit the growth of brain tumor–initiating cells. Moreover, niacin treatment of intracranial mouse models of glioblastoma increased monocyte and macrophage infiltration into the tumors, stimulated antitumor immune responses, and extended the animals' survival, especially when combined with the chemotherapeutic drug temozolomide.